Australian Government
Bureau of Meteorology

The Centre for Australian Weather and Climate Research
A partnership between CSIRO and the Bureau of Meteorology

CSIRO

The Simple Carbon-Climate Model: SCCM7 Technical Documentation

Ian N. Harman and Cathy M. Trudinger

CAWCR Technical Report No. 069

April 2014

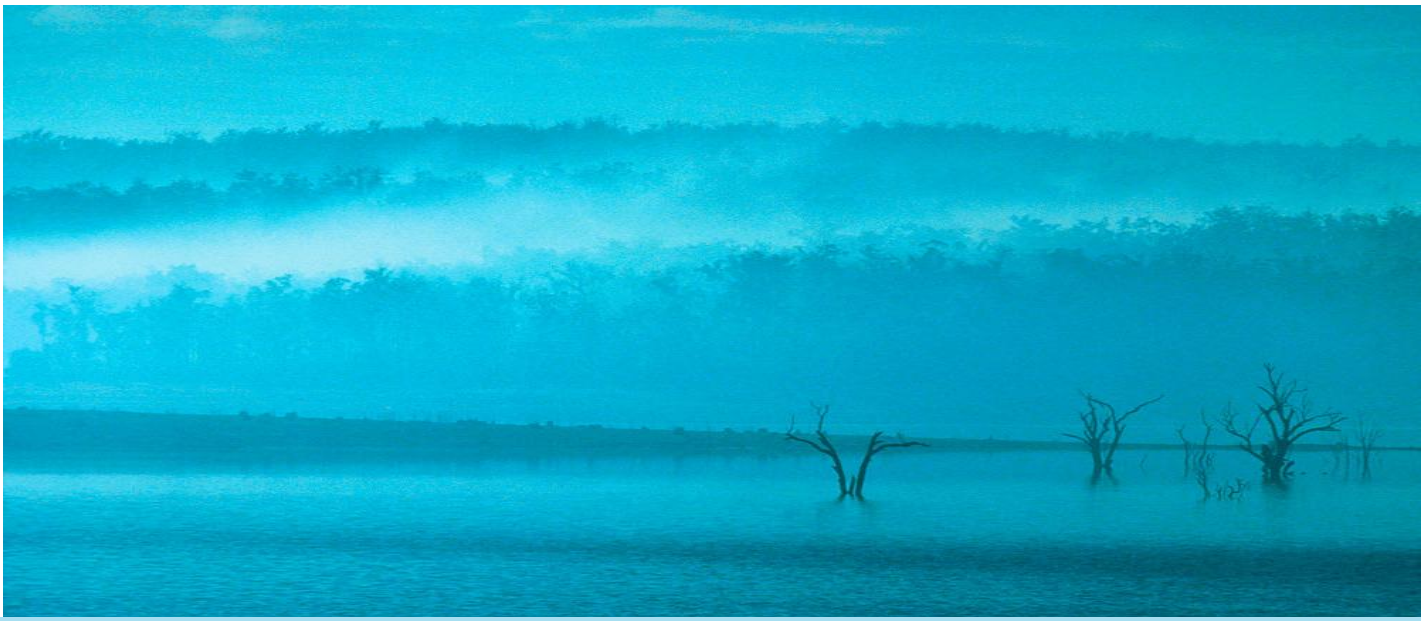

www.cawcr.gov.au

The Simple Carbon-Climate Model: SCCM7 Technical Documentation

Ian N. Harman and Cathy M. Trudinger

Centre for Australian Weather and Climate Research (CAWCR),
CSIRO Marine and Atmospheric Research, Canberra, ACT, Australia, 2601

CAWCR Technical Report No. 069

April 2014

ISSN: 1835-9884

National Library of Australia Cataloguing-in-Publication entry

Authors:	Ian N. Harman and Cathy M. Trudinger
Title:	The Simple Carbon-Climate Model: SCCM7 Technical Documentation.
Edition:	CAWCR Technical Report No. 069
ISBN:	9781486302628
Notes:	Includes bibliographical references and index.
Subjects:	Carbon cycle (Biogeochemistry) Greenhouse gases. Atmospheric carbon dioxide.
Dewey Number:	577.144

Enquiries should be addressed to:

Dr. Ian Harman,
CSIRO Marine and Atmospheric Research,
FC Pye Laboratory,
GPO Box 3023,
Canberra, ACT, 2601
AUSTRALIA

ian.harman@csiro.au

Copyright and Disclaimer

All images reproduced in grayscale. A colour version of CAWCR Technical Report No.069 is available online: http://www.cawcr.gov.au/publications/technicalreports.php

Contents

List of Figures

List of Tables

EXECUTIVE SUMMARY

SCCM – the Simple Carbon-Climate Model – is a deterministic model for the globally averaged carbon cycle and climate system. It comprises representations of the carbon, methane, nitrous oxide and other long-lived greenhouse gas mass balances in the Earth system and for the evolution of the global mean near-surface air temperature. The model is designed for when broad scale information about the carbon-climate system is needed within other applications, for example climate change policy analysis or integrated assessment. This report documents updates to the formulation, calibration and operation of SCCM for version SCCM7 and presents some initial, broad scale, results.

1 INTRODUCTION

The Simple Carbon-Climate model (SCCM) (Harman et al. 2011; Raupach et al. 2011a,b) is a member of the set of highly simplified one-dimensional energy and mass balance models for the Earth System (e.g. Wigley 1991; Joos et al. 1996; Good et al. 2011; Meinshausen et al. 2011a,b). It seeks to capture the robust long-term dynamics of the coupled carbon cycle and climate system at a globally integrated level and in a simple form. As carbon is not the only driver of the global climate system additional components such as atmospheric methane, nitrous oxide and aerosols are also included. By maintaining the simplicity of formulation of the model, the unavoidable uncertainties associated with complex systems can more easily be analysed, quantified and understood.

A series of developments have been undertaken to SCCM concentrating on extensions to its flexibility, completeness and calibration. This report concentrates on the scientific basis of the updated SCCM7 and its modes of operation. The report is structured as follows: In Section 2 we outline the scientific basis and mathematical formulation of the updates to SCCM7. In Section 3 we document some efforts to calibrate SCCM and consider some projections of future climate for the IPCC-AR5 standard scenarios. Section 4 updates how the model is written and structured, the different configurations available and how it is used. Finally, we provide a brief summary and tables for the terminology and variables used. For the most part the contents of this report do not affect how SCCM7 operates within CSIRO's integrated assessment model GIAM (Gunasekera et al. 2008; Harman et al. 2008). This report builds on, and should be read in conjunction with, the earlier technical documentation for SCCM (Harman et al. 2011).

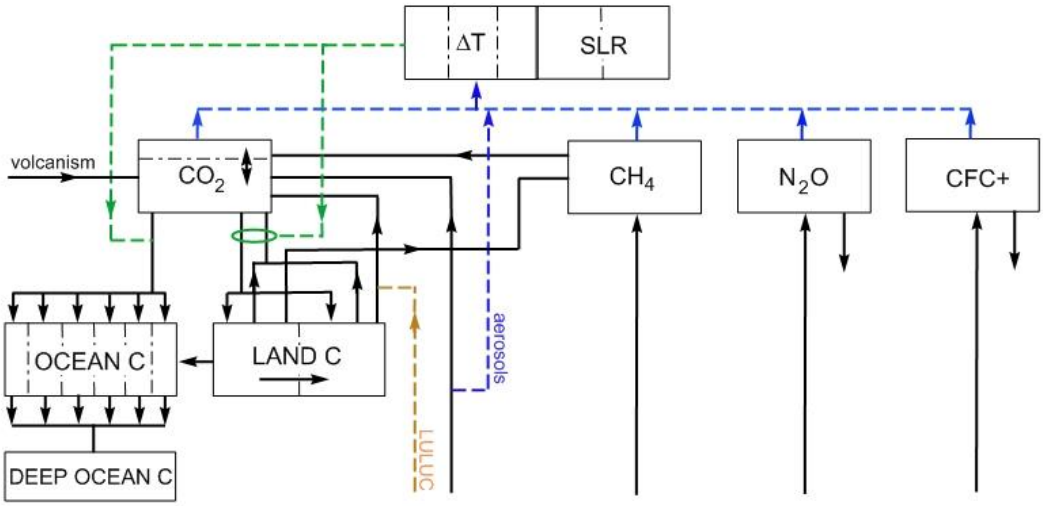

Fig. 1 Schematic of the general structure of SCCM (adapted from Harman et al. 2011). Boxes indicate the state variables, solid lines are fluxes of material and dashed lines influences. Further details are given in the text. The primary updates to the structure of SCCM described by Harman et al. (2011) are the partitioning of the atmospheric CO_2 state variable into two, the addition of the sea-level rise (SLR) variables and the additional long-lived greenhouse gas state (CFC+) variables. Not all components are required for every application. Additional components ($^{13}CO_2$ and $^{14}CO_2$ cycles) are available or in development.

2 THE SIMPLE CARBON-CLIMATE MODEL (SCCM7)

The Simple Carbon-Climate Model (SCCM) is a quantitative model for the globally-averaged carbon cycle and climate system. Its primary aim is to take time series of estimates of emissions (either anthropogenic or total) of greenhouse gases (GHGs) and calculate the globally-averaged concentration of these gases, and the resulting changes in global radiative forcing and near-surface air temperature. Other models in this general category include MAGIC-C (Wigley 1991; Meinshausen et al. 2011a,b) and the Bern-CC model (Joos et al. 2001).

SCCM calculates the variation with of various state variables in the state vector, **x**. Typical state variables include the atmospheric concentration of CO_2, other greenhouse gases (GHGs) and the change in the near-surface air temperature (approximated in SCCM by the change in the temperature of the oceanic mixed layer given that the ocean heat capacity is many times greater than that of the atmosphere). Model equations for the evolution of the state vector over time are written as differential equations ($\mathrm{d}\mathbf{x}/\mathrm{d}t = \ldots$) and solved numerically.

The model can consider a number of different GHGs (CO_2, CH_4, N_2O and number of other long-lived GHGs – denoted by CFC+). These can be modelled at the same time or subsets can be chosen if the application demands this. Figure 1 shows a general linkage diagram for a standard (GIAM) configuration of SCCM, with boxes indicating state variables, solid lines fluxes and dashed lines influences. A major advance with SCCM7 is the extension of the capability to use observations of radiative forcing (real or synthetic) in place of SCCMs

endogenously derived values. Hence the temperature component can now be forced with a time series of radiative forcing, not the endogenous gas concentration time series, and be assessed independently of the carbon-cycle, chemistry or aerosol parameterisations.

The following sections provide details of the updated and extended formulation of SCCM7.

2.1 Updates to the Carbon Cycle

SCCM modelled the carbon cycle as the exchange of mass between the three primary active stocks of carbon in the Earth system – the atmosphere, the mixed layer of the ocean (including the marine biosphere) and the terrestrial biosphere. The perturbation to the deep ocean stock of carbon was included in order to satisfy conservation, as was a connection between the carbon dioxide and methane cycles. Simple parameterisations of the exchange between the three stocks were used to determine gross features of future projections of the carbon cycle.

The parameterisation of the carbon-cycle within SCCM7 is largely unchanged from that of SCCM4. Developments, still ongoing, of the representation of the cycles of the carbon isotopes (the $^{13}CO_2$ and $^{14}CO_2$ cycles) has required one minor update to the parameterisation of the main carbon cycle. The perturbation from preindustrial conditions to the atmospheric stock of carbon (as CO_2) is now partitioned into two pools representing 'tropospheric CO_2' (C_{TROP}) and 'stratospheric CO_2' (C_{STRAT}) with each stock (in GtC) having separate dynamics. The evolution of the two pools is modelled as

$$\frac{dC_{TROP}}{dt} = F_{CO2\_FOSS} + F_{CO2\_LUC} - F_{COS\_AS} - F_{CO2\_AB} + F_{CO2\_CH4} + F_{VOLC} + F_{CO2\_ST} \qquad (1)$$

and

$$\frac{dC_{STRAT}}{dt} = -F_{CO2\_ST} \qquad (2)$$

where the fluxes/emissions have the same meaning as in Harman et al. (2011) and are time dependent. The total perturbation to the stock of atmospheric CO_2 (CO2) is given by the sum of the two pools and obeys the same rate equation as that in SCCM4. The additional flux term in Eqs (1) and (2), F_{CO2_ST} represents the quantity of carbon exchanged between the pools and is given by

$$F_{CO2\_ST} = \left(C_{STRAT} - \frac{C_{TROP}\, f_{STRAT}}{1 - f_{STRAT}} \right) / \tau_{STRAT} \qquad (3)$$

where f_{STRAT} is fraction of the atmospheric stock of CO_2 residing in the stratosphere in preindustrial conditions (i.e. taking a value between 0 and 1) and τ_{STRAT} is a stratospheric turnover timescale (of typical magnitude 4 years). As the two stocks represent perturbations to the preindustrial conditions both are initialised to zero and consequently F_{CO2_ST} also represents a perturbation flux. The sign of F_{CO2_ST} acts to reduce the differences between the perturbation stocks C_{TROP} and C_{STRAT} that evolve due to anthropogenic emissions and other perturbations to the modelled carbon cycle. Surface CO_2 observations should be compared to C_{TROP}.

Within SCCM the atmospheric stock of carbon is converted to a near-surface concentration of CO_2, e.g. for use in calculating the air-sea and air-land fluxes, through a conversion factor $r_{CO2\_ppmGtC^{-1}}$. The value used for this factor applies to whole atmosphere whereas surface concentrations reflect only the troposphere. Consequently the near-surface concentration of CO_2 is adapted to

$$\mathrm{CO2_{TROPppm}} = \mathrm{CO2_{preppm}} + C_{TROP}\frac{r_{CO2\_ppmGtC^{-1}}}{1 - f_{STRAT}} \tag{4}$$

where $\mathrm{CO2_{preppm}}$ is the preindustrial value for the tropospheric concentration of CO_2 (in ppm) and $r_{CO2\_ppmGtC^{-1}} = 0.4695$ ppm GtC^{-1} is the conversion factor. $\mathrm{CO2_{TROPppm}}$ is used in place of $\mathrm{CO2_{ppm}}$ in the parameterisations for the Net Primary Productivity and air-biosphere flux (Eqs 12-20 in Harman et al. 2011) and for the parameterisation of the air-sea flux (Eq 3 in Harman et al. 2011).

Note that if f_{STRAT} =0 then Eqs (1-4) revert to the original parameterisation of the carbon cycle described in Harman et al. (2011).

2.2 Updates to the Long-Lived Greenhouse Gas Component

SCCM4 included simple representations of the chemical cycles of two, dominant, long-lived greenhouse gases, CFC-11 and CFC-12. As the international measures to control emissions of these gases continue, increased attention is being paid to other powerful, long-lived greenhouse gases. To facilitate analyses of the evolution of these other gases SCCM7 an additional HFC component has been added which considers *up to* 7 long-lived GHG. (Nominally these gases are CFC-11, CFC-12, HCFC-22, HFC-23, HFC134a, SF6 and PFC-14 with the latter 5 gases explicitly covered by the integrated assessment model GIAM – Harman et al. 2008). For each gas its chemistry and its radiative impacts are characterised by a single lifetime, a single preindustrial value and a single radiative efficiency and, hence, the seven gases can be interchanged with any other gas which has these attributes[1]. The quantity of these gases in the atmosphere evolves according to the rate equation

$$\frac{\mathrm{d}X_{\mathrm{pre}}}{\mathrm{d}t} + \frac{\mathrm{d}\Delta X}{\mathrm{d}t} = \frac{\mathrm{d}\Delta X}{\mathrm{d}t} = F_X - \frac{\Delta X + X_{\mathrm{pre}}}{\tau_X} \tag{5}$$

where X_{pre} denotes the preindustrial atmospheric quantity of the gas (usually in kt and usually 0), ΔX is the perturbation to the quantity of gas (in the same units as X_{pre}), F_X represents the *total* emissions of gas *X* including natural, perturbations to natural and anthropogenic sources, and τ_X is the lifetime of gas *X* in the atmosphere (dictated by chemical or photo-chemical processes). If $X_{\mathrm{pre}} \neq 0$ then this implies that there must be a non-zero natural source of gas *X* (e.g. for PFC-14)

For each gas, the contribution to the total radiative forcing is given by

[1] Within the code CFC-11 and CFC-12 in the new HFC model are denoted dCFC-11 and dCFC-12 to avoid confusion.

$$\mathrm{RF}_X = r_{\mathrm{eff}X}\, r_{X\_\mathrm{pptkt}^{-1}} \left(X_{\mathrm{pre}} + \Delta X\right) \tag{6}$$

where $r_{X\_\mathrm{pptkt}^{-1}}$ is a conversion factor from (usually) kt of gas to ppt, and $r_{\mathrm{eff}X}$ is the radiative efficiency of the gas *X* (in corresponding units of $\mathrm{Wm}^{-2}\mathrm{ppt}^{-1}$).

As per Harman et al. (2011), both 'total' and 'perturbation' options are included for the representation of the chemistry of gas *X*. However all long-lived gases considered operate with same option in each simulation. Similarly the radiative forcing due to the long-lived gases can be included or neglected in the temperature component of the SCCM through the use of the parameter set s_{fi} (Eq 40 in Harman et al. 2011). Again, however, the radiative forcing from either all or none of the long-lived GHGs considered can be included. Partial inclusion can be facilitated by running SCCM multiple times with different gases active.

2.3 Extension to include Sea-Level Rise

Global sea-level rise (SLR) is one of the important metrics of climate change – from both a biophysical and policy perspectives (IPCC 2013). Changes to sea-levels are comprised of several factors with the two important components being expansion/contraction of the ocean water due to changes in density (i.e. due to changes in temperature and/or salinity) and changes in the volume of water in the oceans resulting from changes in storages in land, ice sheets, glaciers and the atmosphere. The former impacts are well-understood though spatially and temporally variable and linked to changes in the ocean circulations. The latter impacts are less well understood with the primary source of uncertainty arising from uncertainties in ice-sheet dynamics (e.g. Church et al. 2009; IPCC 2013).

Three representations for sea-level rise are included within SCCM7 – each has their own attributes, strengths and weaknesses. The first option, slrmodelchoice='accc', parameterises global sea-level rise through the use of a 2-term impulse response function based on globally-averaged radiative forcing, *RF*. This response function was used in 2002 for the default cases in the UNFCCC Assessment of Contributions to Climate Change (ACCC) (den Elzen et al. 2002). The impulse response function was fitted to the 950 year, thermal expansion run of the HadCM3 Earth System model. Specifically, the integral form

$$\mathrm{SLR}(t) = \frac{\mathrm{SLR}_{\mathrm{eq}}}{RF_{\mathrm{eq}}} \int_0^t RF(t')R_{SLR}(t-t')\mathrm{d}t' \tag{7}$$

is converted to AR1 form (Wigley 1991, Enting 2007)

$$\frac{d\mathrm{SLR}_i}{\mathrm{d}t} = \frac{\mathrm{SLR}_{\mathrm{eq}}}{RF_{\mathrm{eq}}}\; RF(t)\, a_{\mathrm{SLR}i} - \alpha_{\mathrm{SLR}i}\, \mathrm{SLR}_i \qquad i = 1,2 \tag{8}$$

with $\mathrm{SLR}=\mathrm{SLR}_1+\mathrm{SLR}_2$, $\mathrm{SLR}_{\mathrm{eq}} = 4.7395$ m and RF_{eq} =7.0 Wm^{-2} being the equilibrium sea-level rise and radiative forcing at 4× preindustrial CO_2 concentrations. The coefficients of the response function are a_1=0.96677, a_2=0.03323, τ_1=1700.2 y, τ_2=33.788 y (den Elzen et al. 2002). This option is well calibrated against a long data set however any weaknesses in the HadCM3 ocean or, particularly, ice sheet models inevitably feed into this option through the

calibration of the response function (i.e. not all contributions to sea-level rise are necessarily included).

The second option, slrmodelchoice='vermeer', parameterises SLR via a single rate equation based on globally-averaged near-surface temperature and its rate of change (Vermeer and Rahmstorf 2009, 2010). It has been calibrated using observations of sea-level rise and temperature during the period 1880-2000. The rate equation for SLR takes the form

$$\frac{d\mathrm{SLR}}{\mathrm{d}t} = a\left(T - T_{\mathrm{pre}}\right) + b\frac{dT}{\mathrm{d}t} \tag{9}$$

with a=0.0056 $\mathrm{mK^{-1}y^{-1}}$, b=-0.049 $\mathrm{mK^{-1}}$ and T_{pre} the preindustrial global mean near-surface temperature. As this option is based around observations it includes all contributions to sea-level rise however the relatively short and sparse data record available does imply that components of the Earth system that will become active in the longer term (but have yet to be so) are not captured in the calibration and statistical uncertainty in the coefficients *a* and *b* will be noticeable.

The third option, slrmodelchoice='jevrejeva', parameterises SLR via a single rate equation based on globally-averaged radiative forcing (Jevejeva et al. 2012). The rate equation is

$$\frac{d\mathrm{SLR}}{\mathrm{d}t} = \left(\mathrm{SLR_{eq}} - \mathrm{SLR}\right)/\tau_{\mathrm{SLR}} \tag{10}$$

with

$$\mathrm{SLR_{eq}} = a\,RF + b \tag{11}$$

and because the derivative depends on SLR itself we cannot assume the pre-industrial sea-level rise $\mathrm{SLR_{pre}}$=0 m. Here $\mathrm{SLR_{eq}}$ is the equilibrium sea-level rise as a function of current radiative forcing and τ_{SLR} is a sea-level response time scale. Jevrejeva et al. (2012) give only probability density functions for the parameters, not best values, but the median values for one of their three reconstructions (GRT_2005) are $\tau_{\mathrm{SLR}} = 99$ y, *a*=0.3 $\mathrm{mW^{-1}m^2}$, b=0.3 m, $\mathrm{SLR_{pre}}$=-0.4 m (however, being median values from the pdfs, they may not be a consistent parameter set). Without consistent parameter sets we are reluctant to recommend this option. This option is also based on observations therefore also includes all contributions to sea-level rise and the same comments around uncertainty made above also apply.

The Vermeer and Rahmstorf (2009) and Jevrejeva et al. (2012) options differ in their inclusion of the effect of water stored on land. Vermeer and Rahmstorf (2009) included reservoir construction but not the potentially cancelling effects of groundwater mining and urbanisation, while Jevrejeva et al. (2012) included no land contributions. Finally we specifically note that simple models for sea-level rise tuned on past sea-level rise give future sea-level rise (up to) 3 times bigger than in the IPCC model projections (Grinsted et al. 2010 – see Section 3).

2.4 Extension to operate in Carbon Dioxide-equivalent Mode

Figure 1 illustrates the coupled nature of many of the components of SCCM, particularly the carbon cycle and temperature components. Calibration/validation of SCCM7 and its sub-components is then complicated as weaknesses and/or errors in one component of the model can manifest in other components and lead to an incorrect assessment because of compensating errors. SCCM4 permitted the use of observations of atmospheric constituents and temperature, in place of the endogenous quantities, to drive other components of SCCM, which assists with this issue. However, SCCM4 also parameterised the radiative forcing due to aerosols in terms of the emissions of fossil fuels. This link, uncertain in the past and more so in the future, prevents the complete separation of the carbon cycle and the temperature components from the emissions, or from each other. This separation is important if we wish to use output from General Circulations Models (GCMs) or Earth System Models (ESMs), driven by radiative forcing time series, as part of the calibration/validation process in our efforts to ensure that SCCM replicates the behaviour of the more complex Earth System models.

SCCM7 has been extended, in part to address this issue, and can now accept time series of radiative forcing to be used to force the temperature component – in place of the time series of CO_2, CH_4, N_2O, the other GHGs and aerosol forcing. The carbon cycle and atmospheric chemistry do not then impact on the evolution of the temperature. The time series of radiative forcing is supplied to SCCM7 as a time series of CO_2-eq through the option tempco2choice='co2e'. It is important to ensure that the equations and parameter values used to generate the, now exogenous, CO_2-eq time series match those used within SCCM used to convert between CO_2 and radiative forcing (Eq 35 in Harman et al. 2011).

2.5 Extension to include Parameter Estimation via PEST

SCCM4 included the genetic algorithm code from Haupt and Haupt (2004) as an endogenous method to objectively estimate parameter values for SCCM. We now also use SCCM with the Levenberg-Marquardt package PEST (Doherty et al. - http://www.pesthomepage.org) as a second objective method to optimise parameter values and the associated uncertainty. SCCM writes out model variables corresponding to the calibration observations in a format suitable for PEST. In addition to instantaneous values of model variables, we also allow the use of averages over time, as well as model variables convolved with a Greens function from a model of firn diffusion and bubble trapping (Trudinger et al. 2013), to allow SCCM output (atmospheric concentrations in particular) to be smoothed in a way similar to ice core measurements (Trudinger et al. 2003).

3 CALIBRATING SCCM7 TEMPERATURE COMPONENT

SCCM is founded on the basic scientific principles of conservation of mass and energy; however, it does not include representations of the many physical processes acting within the climate system. Instead SCCM can be considered to be a collection of statistical relationships or parameterisations designed to capture the outcomes of those processes at the global scale. The various components of SCCM must, therefore, be carefully calibrated against observations and other modelling approaches where the relevant physical processes are directly (and correctly) represented. In this section we outline the methodology used to calibrate the temperature response function against more complex models of the climate system, specifically the suite of General Circulation Models (GCMs) and Earth System Models (ESMs) involved in the 5th Coupled Models Inter-comparison Project (CMIP5) (Taylor et al. 2012). This suite of models represents the current state of knowledge and best practice in climate modelling as of 2012-2013. Other, more in depth, analyses of the CMIP5 including the possible representation of the complex GCMs and ESMs by simpler models have been reported (e.g. Bodman et al. 2013; Good et al. 2011, 2013; Joos et al. 2013). However given the unique formulation and roles SCCM fulfils it remains important that such a calibration exercise is undertaken specific to SCCM.

3.1 Temperature Component of SCCM

The temperature component of SCCM provides information about changes to the globally and annually averaged temperature of the mixed layer of the ocean (in K) given a time series of radiative forcing (in Wm^{-2}) (Harman et al. 2011). This temperature is used within the remainder of SCCM as a proxy for the globally and annually averaged near-surface air temperature, the commonly used metric in many analyses of global climate change. The temperature component is expressed in the AR1-form of a response function (Wigley 1991; Enting 2007) whereby the change in temperature, ΔT, is given by the system of linear first order differential equations

$$\Delta T = \sum_{i=1}^{n} T_i \tag{12}$$

where

$$\frac{\mathrm{d}T_i}{\mathrm{d}t} = RF(t)\, C_{sens}\, a_i\, \alpha_i - \alpha_i T_i \tag{13}$$

subject to

$$\sum_{i=1}^{n} a_i = 1 \tag{14}$$

where $RF(t)$ is the prescribed scenario for the globally averaged radiative forcing. The coefficients a_i (partitions) and α_i (inverse time scales) define the temporal characteristics of the response function and the parameter C_{sens} quantifies the overall magnitude of the temperature response to a change in radiative forcing.

Calibrating SCCM then requires the parameters C_{sens}, a_i and α_i to be determined using information from GCM simulations. A response function with *n*=2 or 3 terms has been found to be sufficient to represent most GCMs but there are no technical reasons why additional terms cannot be included. Once calibrated SCCM will then provide an *estimate* of the global temperature trajectory under a given scenario of radiative forcing as would be given by the basis GCM. However, regional correlations, especially between radiative forcing and climate change, the difficulties of calibration in the face of climate variability and nonlinearities in the climate system prevent exact replication. Meinshausen et al. (2011a,b) note that such simple representations of the climate system inevitably cannot replicate path-dependent features in the climate system (e.g. tipping points) and that, consequently, different calibrations may be needed based on the trajectory of radiative forcing.

3.2 Calibration using CMIP5 Model Output

The CMIP5 is a large collaborative project involving many climate scientists, climate change scientists and climate impact scientists (Taylor et al. 2012). Central to this effort is a co-ordinated set of climate simulations undertaken by the climate modelling groups and universities around the globe. For the purposes of calibrating SCCM three key simulations, undertaken by all groups, are used, namely

A. the preindustrial control simulation (usually many thousands of years long)

B. the abrupt 4× CO_2 control simulation (usually 150 years long)

C. the 1%-per-year increasing CO_2 control simulation (usually 140 years long).

The two experimental control simulations (B & C) are used here because, as outlined in more detail below, these scenarios permit analytical solutions to the equations (12). The analytical solutions, however, are for the *temperature change* and not the temperature itself (as given by the model). Consequently the preindustrial control simulation is needed so that the change in temperature can be calculated. Given time series of the globally and annually averaged temperature change, parameter estimation techniques can then be used to determine the 'best-fit' parameter values for each of the GCMs considered.

Temperature changes are calculated as the difference between the control simulation and the preindustrial control. The differences are calculated for every month and on the grid of the OAGCM before being averaged up to global and annual averages.[2] The control simulations are conventionally initialised using fields from the preindustrial control. Consequently only part of the preindustrial control simulation is used so that it and the control simulation are referenced to the same zeroth year. This method (in contrast to calculating a long-term climatology from the preindustrial control and subtracting) ensures that long-term modes of climate variability, simulated by the OAGCM and locked in via the initial conditions, are not present in the temperature change values deduced. Algebraically the time series of the temperature change for each of the control simulations is given by

[2] Ideally temperature changes would be calculated on the time step of the model, however output for these scenarios is only provided as monthly averages.

$$\Delta T_{CS}(t) = \sum_k \sum_l \sum_m w(k,l,t_m)\,[T_{CS}(k,l,t_m) - T_{PI}(k,l,t_{m+OFF})] \qquad (15)$$

where T_{CS} and T_{PI} are fields of monthly, GCM grid based near-surface temperature from the control and preindustrial control simulations respectively. *k*, *l* and *m* are the longitude, latitude and time indices, *OFF* gives the time index to ensure a consistent zeroth year and *w* are the weightings by surface area and length of month needed to provide the estimate of a true spatial and temporal average from discretized data.

The time series of radiative forcing applied within for the two control simulations (4x and 1% denoting control simulations B and C respectively) are

$$RF_{4\times}(t) = \begin{cases} 0 & t \le 0 \\ A\ln(4) & t > 0 \end{cases} \qquad (16)$$

and

$$RF_{1\%}(t) = \begin{cases} 0 & t \le 0 \\ A\ln(1.01^t) = A\,t\ln(1.01) & t > 0 \end{cases} \qquad (17)$$

where *t* gives time (in years) from the start of the forcing. The parameter *A* quantifies the radiative forcing per unit change in atmospheric CO_2 and does itself vary between GCMs (typically taking a value of approximately 5.35 Wm^{-2}). For the purposes of the calibration of SCCM, however, *A* and C_{sens} always appear as product and hence $A\,C_{sens}$ is the parameter which is estimated.

The solutions to (13) given the radiative forcing are

$$\Delta T_{4\times}(t) = A\,C_{sens}\ln(4)\left(1 - \sum_{i=1}^{n} a_i e^{-\alpha_i t}\right) \qquad (18)$$

and

$$\Delta T_{1\%}(t) = A\,C_{sens}\ln(1.01)\left(t - \sum_{i=1}^{n}\frac{a_i}{\alpha_i} + \sum_{i=1}^{n}\frac{a_i}{\alpha_i}e^{-\alpha_i t}\right) \qquad (19)$$

The climate sensitivity, $\Delta T_{2\times}$, is related to *A* and the response function parameters as

$$\Delta T_{2\times} = A\,C_{sens}\ln(2) \qquad (20)$$

For ease of comparison to other studies further discussion of this parameter will be in terms of $\Delta T_{2\times}$.

The parameters in the response function appear in nonlinear combinations within (18) and (19). Furthermore the solutions cannot be readily transformed into a linear system (in the parameters or combinations of parameters). Calibration of the response function parameters is therefore non-trivial and a step-wise process has consequently been implemented as described next.

In common with many parameter estimation algorithms the objective basis for the calibration is to find the combination of parameter values which minimises an objective function, J, defined as the mean of the squares of the differences between the model and a set of 'observations'. Suppose we have $n_{4\times}$ observations of ΔT from the abrupt 4× CO_2 control simulation and $n_{1\%}$ observations from the 1% per year increasing CO_2 control simulation then J is given by

$$J(\boldsymbol{P}) = n_{4\times}^{-1}\sum_{j=1}^{n_{4\times}}\left(\Delta T_j - \Delta T_{4\times}(\boldsymbol{P},t_j)\right)^2 + n_{1\%}^{-1}\sum_{k=1}^{n_{1\%}}\left(\Delta T_k - \Delta T_{1\%}(\boldsymbol{P},t_k)\right)^2 \qquad (21)$$

where $\boldsymbol{P} = [AC_{sens}, a_1, \ldots, a_{n-1}, \alpha_1^{-1}, \ldots, \alpha_n^{-1}]$ is the vector of independent parameters. Calibration is carried out on the time scales, α_i^{-1}, and not their reciprocals for numerical reasons. A search algorithm proceeds as follows

1. An initial, plausible, estimate for $\boldsymbol{P}=\boldsymbol{P}_0$ is provided and the initial value of $J(\boldsymbol{P_0})$ determined.

2. For each parameter, P_i, in turn

   a. apply positive and negative increments to P_i, recalculate $J(P_i|\boldsymbol{P}_{\neq i})$ and determine the local slope in J.

   b. apply further increments to P_i in the direction of reducing J, recalculating J each time, until J subsequently increases – a local minimum in $J(P_i|\boldsymbol{P}_{\neq i})$ has been found.

   c. $\boldsymbol{P}$ is updated using the value of P_i at the local minimum.

3. Repeat around all the elements of the parameter vector until further reduction in J is not possible when changing any parameter value. The calibrated value for $\boldsymbol{P} = \widehat{\boldsymbol{P}}$ has been found.

4. The calibrated value of $\widehat{\boldsymbol{P}}$ is checked for realisability – all parameters need be greater than zero.

The search algorithm above finds the value for $\boldsymbol{P}$ at a local minimum in J not necessarily at the global minimum. The variability in the observation (GCM) data implies that multiple local minima for J are possible. Consequently different initial estimates for $\boldsymbol{P}$, different ordering of the searches and different increments may lead to different final solutions. For the purposes of calibrating SCCM these implementation/algorithm issues are unlikely to be problematic, especially if adequate uncertainty estimates are calculated, however for some applications of SCCM (e.g. policy applications where discussions around the climate sensitivity have become important) further consideration of the details of the calibration will be needed.

The data used encompasses climate variability arising from a range of physical processes, as represented within the GCM, each with their own inherent times scales. The calibration attempts to discern the larger, global scale signal given this inherent variability. However, as with many issues surrounding climate modelling, limited data exists and consequently there is a strong element of contingency to the eventual results. For example, most of the modelling groups have performed only one abrupt 4× CO_2 and one 1% per year control simulation. It is possible, indeed likely, that if another simulation were undertaken and used to calibrate the response function a different best fit parameter combination would be determined. This,

together with the issues around multiple minima in the objective function, the numerical issues concerning the search algorithm itself and the possibility of correlation between the eventual parameter values, implies that multiple solutions are possible, each of which is physically plausible. This issue of *equifinality of the parameter vector* is inherent in nearly all cases when data from complex models are used to calibrate simpler models, not solely within the climate arena. Consequently, if for no other reason, it is important to quantify the uncertainty around the 'best-fit' parameter vector determined.

As a formal parameter estimation technique (e.g. PEST or the GA) has not been used, formal error estimates are not easily determined. Instead estimates of the uncertainties around $\tilde{\boldsymbol{P}}$ have been quantified using an ensemble of partial samples. 50 subsamples of size 24[3] were taken randomly from the available GCM data and used to determine additional estimates of the response function parameters. Error estimates (around the central estimate for parameter values obtained using all data) are then provided from the covariance matrix of the resultant ensemble and the impact of parameter uncertainty can be propagated through SCCM, via Monte-Carlo simulation, to assess the impact on projections of temperature, sea level rise and other important state variables.

3.3 Exemplar SCCM7 Temperature Component Calibrations

CMIP5 comprises a large range of modelling groups and individual Earth System and General Circulation models. We illustrate the calibration technique by considering 6 of these models in some detail; the performance against 27 models (all that had reported sufficient results to carry out the calibration by 10/2012) is shown in Appendix B. The 6 models considered are ACCESS1.3 (CAWCR's flagship Earth System Model – Bi et al. 2013; Dix et al. 2013) together with 5 models which undertook at least 3 simulations for three of the Representative Concentration Pathways (RCPs), specifically RCP3PD, RCP4.5 and RCP8.5 – see van Vuuren et al. (2011a) and Taylor et al. (2012).

Figure 2 shows the GCM data (crosses) and fitted SCCM7 three-term calibrations for each of the 6 models. Also shown are the parameter values and value for *J* for the central estimate. For all of these GCMs the calibration successfully manages to reproduce the magnitude and timing of temperatures changes (although this is not universal – see Fig. 6). For two of the models – ACCESS1.3 and CanESM2 – two of the three terms identified possessed identical timescales (and which were near-equal to one of the timescales identified using a two-calibration). Consequently the two identical terms have been combined. While separate timescales have been identified through the calibration these should not be identified with specific physical processes without further careful consideration (Li et al. 2009). There is a tendency for the calibration to systematically underestimate the temperature change from the abrupt $4\times CO_2$ control simulation but underestimate the temperature change from the 1%-per-year increasing CO_2 control simulation (most evident in the MIROC5 calibration). From the information present in the data it is not possible to identify the cause of this tendency – though a nonlinear process(es), such as change in the stratification of the ocean, is (are) the obvious candidate(s).

[3] with no repetition within each subsample: As only 6 independent data are required to quantify the parameters in the response function this subsample of data still provides adequate redundancy for the least squares estimation method.

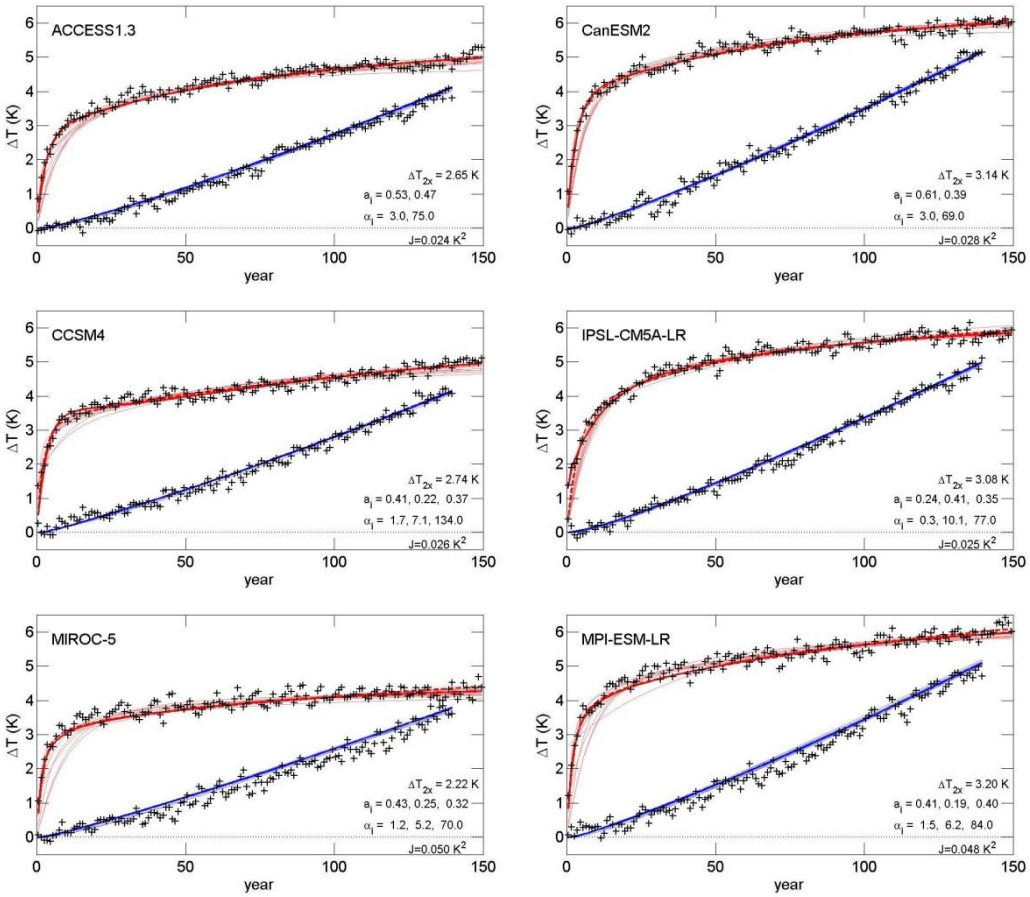

Fig. 2 Exemplar 3 term SCCM temperature component parameter calibrations for 6 GCMs/ESMs. Red lines and associated crosses relate to the abrupt 4×CO2 control simulation; blue lines and associated crosses relate to the 1%-per-year increasing CO2 control simulation. The thin lines give the SCCM projections for each of the 50 member ensemble used to generate uncertainty estimates. The solid thick line gives the central projection obtained by calibration against all data. The dashed line gives an alternate central projection obtained by calibration against all data but using a different numerical search algorithm. The numerical values of the central estimate for the SCCM parameters are given in the bottom right of each panel together with the corresponding value for *J*. For some GCMs the 2-term and 3-term calibrations give identical results.

The ensemble of estimates allows an assessment of the uncertainty in the estimated parameters. These are ensemble (and model) specific however typical values of the standard deviations of the parameters are: 0.1 K around $\Delta T_{2\times}$; 0.1 around a_i; 2 y around α_1; 7 y around α_2; and 10 y around α_3. There are two important consequences of these uncertainty estimates. First, the differences in $\Delta T_{2\times}$ between GCMs are larger than the standard deviation indicating systematic differences in the overall magnitude of response between different GCMs (not solely in timing and climate variability). Second, as the uncertainty of the shorter time scales (α_1 and α_2) approaches or exceeds that of the central parameter estimate these parameters estimates are distributed in a non-Gaussian manner (with consequent impacts on interpretation and statistical inference).

The different parameters in the SCCM7 calibration are constrained by both the GCM data and the functional forms of the expected responses. We therefore expect some interdependence in

the parameter estimates determined. The correlation coefficient r^2 between the 6 parameters quantifies such interdependence. Equation 22 gives an example correlation coefficient matrix calculated for the calibrations to the MPI-ESM-LR model, with the parameters ordered as indicated at the right side. For example the correlation coefficient between $\Delta T_{2\times}$ and α_1 is calculated as -0.27 which indicates that those estimated parameter sets with a larger than average value for $\Delta T_{2\times}$ also (tend) to have a smaller than average estimate for α_1.

$$r^2(\tilde{\boldsymbol{P}}) = \frac{\mathrm{covar}(P_i,P_j)}{\mathrm{var}(P_i,)\mathrm{var}(P_j)} = \begin{pmatrix} 1.00 & -0.10 & -0.20 & -0.27 & -0.04 & 0.67 \\ -0.10 & 1.00 & -0.89 & 0.27 & 0.13 & -0.11 \\ -0.20 & -0.89 & 1.00 & -0.11 & 0.04 & 0.09 \\ -0.27 & 0.27 & -0.11 & 1.00 & -0.34 & -0.21 \\ -0.04 & 0.13 & 0.04 & -0.34 & 1.00 & 0.21 \\ 0.67 & -0.11 & 0.09 & -0.21 & 0.21 & 1.00 \end{pmatrix} \begin{matrix} \Delta T_{2\times} \\ \alpha_1 \\ \alpha_2 \\ \alpha_1 \\ \alpha_2 \\ \alpha_3 \end{matrix} \quad (22)$$

There are two features of particular note in this correlation matrix and which are also shown by the correlation matrices for all examined models. Firstly, many of these coefficient values would be deemed significantly different to zero statistically if they had been determined from a truly independent sample[4]. The potential for the same GCM data to be used within different ensemble members implies that the sample is not independent - nevertheless this does illustrate that the parameters in these calibrations cannot be assumed independent of each other. Second, the largest correlation coefficient occurs between $\Delta T_{2\times}$ and α_3 the longest time scale in the calibration. Importantly, this implies that those estimated parameter sets with higher values of α_3 also have higher values of $\Delta T_{2\times}$. To illustrate this feature of the calibration Fig. 2 also shows results of a calibration using a related, but different, numerical algorithm to determine the central estimate of the parameters values (dashed lines - specifically the search order and starting point differed). This second search algorithm tends to identify (unrealistically) long response time scales (of multiple centuries) in the GCM data but with a larger (by approximately 5%) value for *J*. The subsequent differences in the fits are, however, not easily discerned in the Figure. However, accompanying the longer timescales were (deduced) values for the climate sensitivity approximately 25% larger than those given in Fig. 2 – clearly important for climate policy discussions.

If we accept that GCMs cannot realistically be expected to demonstrate responses with time scales longer than the length of simulation then we also have reason to expect that the longest time scales identified by the calibration will be underestimates of the true responses of the GCM. Hence we should also postulate that the values of the climate sensitivity appropriate to each of the GCMs obtained through the calibration exercise are underestimates (and hence underestimates for that of the climate system itself). Experience using longer run simulations (Li and Jarvis 2009; Harman et al. 2011) confirms this tendency towards the identification of longer time scales with longer simulations. (See also review papers by Knutti and Hegerl (2008) and Rohling et al. (2012) for insights on this topic from modelling and paleo-observation perspectives). For these reasons (systematic correlation and length of simulation) we do not analyse the distributions of the estimated parameter sets further.

[4] With a null hypothesis that the correlation coefficient is zero, a two-sided test and an independent sample of size 50, the critical values which the (absolute value of the) correlation coefficient needs to exceed for the null hypothesis to rejected are 0.2787 at the 5% level and 0.361 at the 1% level. The corresponding values with a one-sided are 0.2353 at the 5% level, 0.3281 at the 1% level and 0.4267 at the 0.1% level (critical values from Table 13 of Lindley and Scott, 1996)

3.4 Simulations of the Representative Concentration Pathways

Any calibration of a model requires additional testing to confirm that the appropriate parameter values have been identified. This is particularly important if equifinality is an issue as is the case for SCCM7. In order to test the calibration of SCCM7 additional projections have been undertaken of the full ensemble of parameter sets for the 4 Representative Concentration Pathways (RCPs). Given the importance of the full suite of greenhouse gases and aerosols in determining the net radiative forcing of the climate the SCCM simulations were undertaken using the CO_2-eq facility in SCCM7. The CO_2-eq time series used to force SCCM were those accompanying the RCPs, i.e. determined by Meinshausen et al. (2011c) using MAGICC-6.

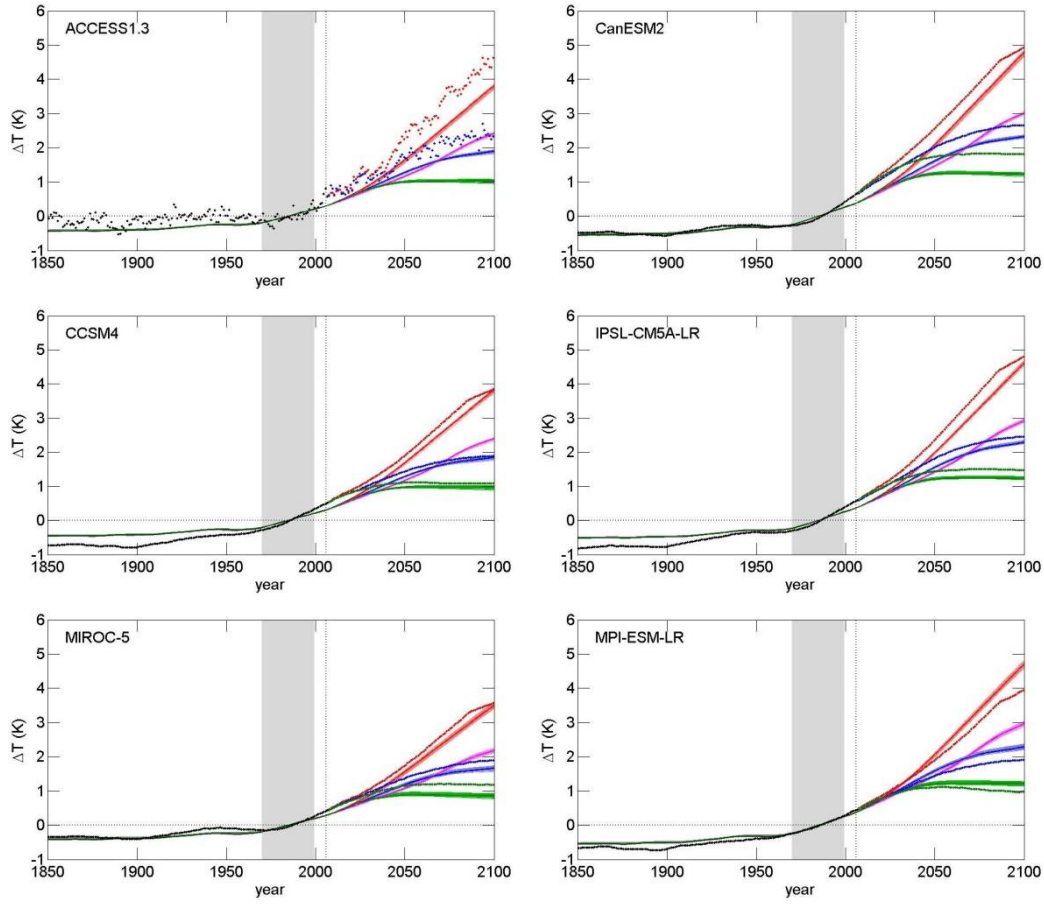

Fig. 3 Comparison of SCCM7 projections against full GCM simulations for the available RCP scenarios. Light coloured bands give the range spanned by the SCCM calibration ensemble, darker coloured lines give the projection using the central calibration. Dots give projections from the GCMs themselves - noting that for GCMs other than ACCESS13 the ensemble average of 3-6 simulations is shown (see text). Green, blue, magenta and red refer to the RCP3PD, RCP4.5, RCP6 and RCP8.5 scenarios respectively. Black refers to the pre-2006 'historical' scenario which is common to the four RCP scenarios. All simulations are referred to the average over the period 1970-1999 (indicated by the shaded box).

Figure 3 shows a comparison between the SCCM7 projections, for each of the 6 models considered in Section 3.3 and for the four RCPs, together with data directly from each of the ESMs and GCMs (where available). For the ACCESS1.3 model the data shown are from one

simulation only; for the other models the ensemble average across the 3-6 simulations carried out is shown. Consequently the GCM data shown from the ACCESS1.3 data are much noisier than from other models.

Overall the performance of SCCM7 to replicate the output of the more complex GCMs is poor. For most of the models and scenarios biases of up to 0.5 K are present and (not shown) these are sufficient to take the SCCM7 projection outside the GCM ensemble. If representative, this degree of inaccuracy would be prohibitive to the use of SCCM7. However a number of factors mitigate this interpretation.

First, while in error, the relative positioning of the 4 RCPs within each scenario set and between the models does reflect that of the GCMs. Second, at least for ACCESS1.3, a significant fraction of the apparent bias can be accounted for through the choice of reference period of 1970-1999. A difference choice of reference period, with a different offset applied uniformly across the simulations, would produce much better agreement. Third, the errors are not necessarily consistent throughout the simulations. For example the match to the CanESM2 model is unbiased during the historical period but notably poor for the future projections. Consistent errors would be expected if an incorrect value for a parameter or parameters were the cause. Fourth there are features in the GCM data which are not evident in the time series of CO_2-eq used to force SCCM. In particular the discontinuity in the slope of the RCP8.5 temperature scenario at 2085 from 5 of the GCMs is neither evident in the CO_2-eq time series used, nor evident in the initial RCP time series of the concentration/emissions of the forcing agents which go into the CO_2-eq time series, as would be expected. Finally, the apparent errors in the SCCM7 projections lie outside the envelope due to choice of parameter sets (this envelope includes the additional set obtained using the different numerical algorithm).

Together these results suggest that the effective CO_2-eq time series generated by the radiation transfer components of these GCMs differs to that used to force SCCM7 (in effect that determined by MAGICC-6) due to differences in the suite of forcing agents considered (e.g. the ACCESS simulations neglected historical stratospheric volcanic aerosol, Dix et al. 2013, unlike MAGICC) and their representation within the GCMs, the impact of averaging forcing and response to regional specific, short-lived agents (aerosols in the main e.g. Lamarque et al. 2013) and/or differences in the radiative transfer calculations themselves. It could also be that the response function form of SCCM7 is insufficient to capture the (path dependent) response of these GCMs (e.g. Meinshausen et al. 2011a, b). Unfortunately it is extremely difficult to generate radiative forcing time series from standard GCM output as the radiative transfer concept assumes that the troposphere, oceans and land are held constant (Forster et al. 2007; IPCC 2013) which is not the case in reality nor within the GCM simulations (see also Appendix C). It is also important to note that a successful calibration against GCM data may not necessarily imply that SCCM7 (or any simple model) will necessarily apply for other scenarios (see Good et al. 2011 for an extensive discussions and references).

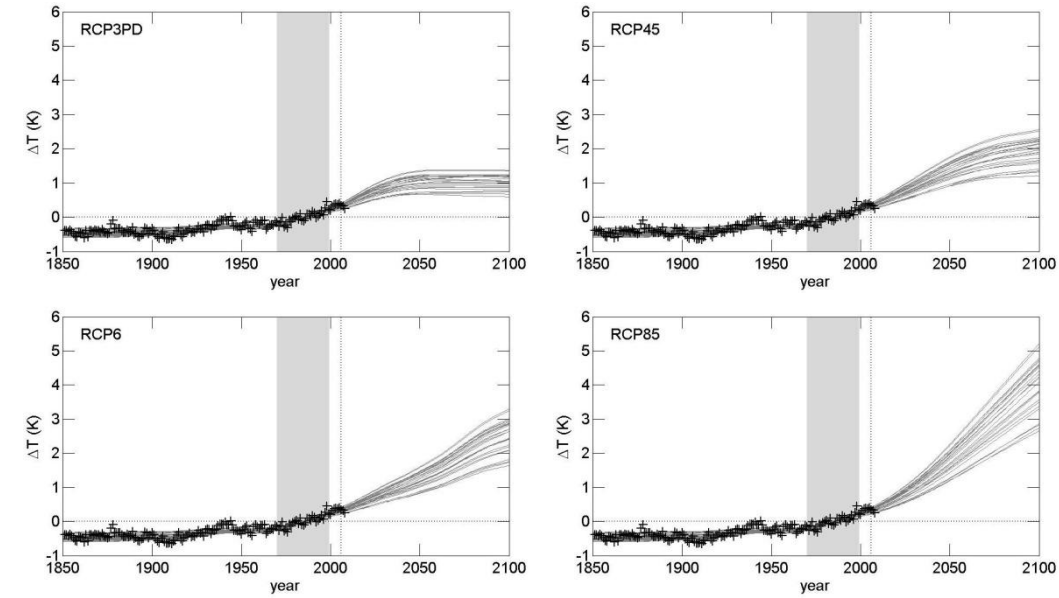

Fig. 4 Projections of the globally-averaged near surface temperature change for each of the four RCP scenarios calculated from the calibrated SCCM7. Thin grey lines show the SCCM projections using the central parameter set for each of the 27 calibrations available. Crosses give the reconstructed observations from Jones et al. (2009). All scenarios and observations referenced to the mean over 1970-1999 (shaded box). The four scenarios deviate in 2006 as indicated by the vertical dotted line.

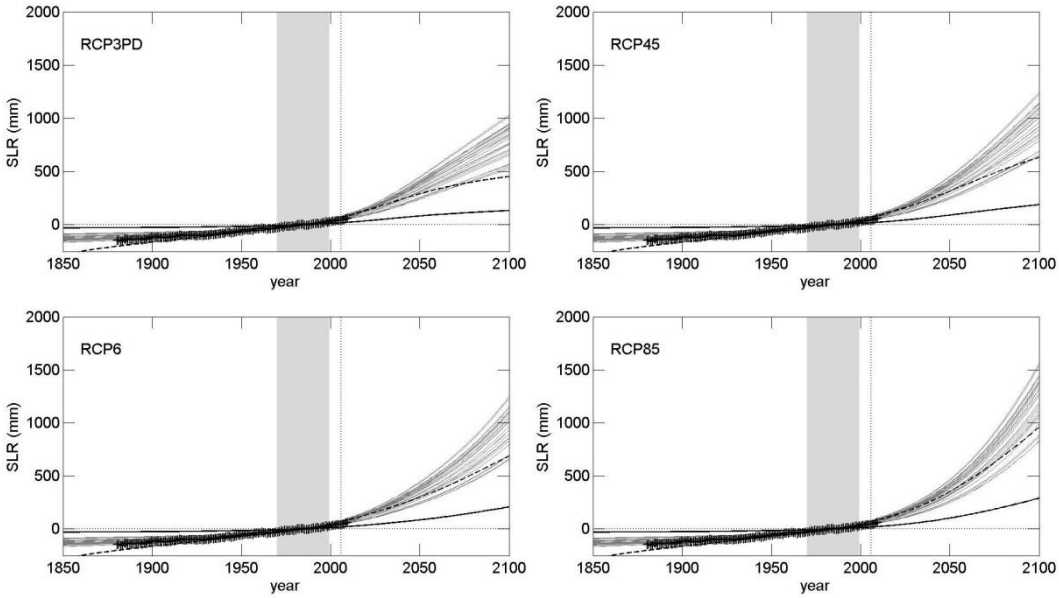

Fig. 5 Projections of the globally-averaged change in sea level for each of the four RCP scenarios calculated from the calibrated SCCM7. Thin grey lines show the SCCM projections for each of the 27 calibrations available using the 'vermeer' parameterisation. Black lines give the projections using the 'accc' (solid) and 'jevrejeva' (dashed) parameterisations which are independent of temperature (and hence calibration). Crosses give reconstructed observations from Church et al. (2011). All scenarios and observations referenced to the mean over 1970-1999 (shaded box). The four scenarios deviate in 2006 as indicated by the vertical dotted line.

Table 1 Comparison between the range in SCCM7 originating from the calibration against different ESMs and GCMs and the *likely*[4] range given by the IPCC-AR5 (2013). Differences in globally-averaged near surface temperature (in K) and sea level rise (in m) are determined for the period 2081-2100 relative to 1986-2005. SCCM ranges are given as the minimum-maximum over the 27 member ensemble. SCCM sea level rise ranges are determined using the 'vermeer' parameterisation in conjunction with the SCCM temperature projections. The projections for sea level rise using the 'jevrejeva' parameterisation lie towards the lower end of these ranges; the projections using the 'accc' parameterisation are approximately 50% of the minimum value quoted (see Fig. 5).

Scenario	SCCM7 ΔT	IPCC-AR5 ΔT	SCCM7 SLR	IPCC-AR5 SLR
RCP3PD	0.5-1.2	0.3-1.7	0.45-0.89	0.26-0.55
RCP4.5	1.1-2.3	1.1-2.6	0.54-1.04	0.32-0.63
RCP6	1.4-2.8	1.4-3.1	0.53-1.02	0.33-0.63
RCP8.5	2.3-4.4	2.6-4.8	0.67-1.26	0.45-0.82

Notwithstanding the above concerns about the performance of the calibration of SCCM7 the ensemble of calibrations can be used to propagate (quickly) the uncertainty due to GCM representation for each of the RCP scenarios. Figures 4 and 5 illustrate the spread in SCCM7 results for the change in globally-averaged temperature and sea level rise, for each of the RCP scenarios, respectively. For the historical period the SCCM envelope is compact (±0.1 K) and captures the magnitude and timing of the observed changes in temperature (Jones et al. 2009). In contrast, the SCCM7 envelope for sea level rise (generated through the use of the 'vermeer' parameterisation with the SLR parameters taking values as stated above i.e. without recalibration) underestimates the observed changes (Church et al. 2009). Sea level rise obtained through the (temperature independent, calibrated against observations) 'jevrejeva' parameterisation slightly overestimates the observed changes, whereas that obtained through the (calibrated against models) 'accc' parameterisation significantly underestimates the observed changes. This tendency is in agreement with the observation of Grinsted et al. (2010) that sea level rise parameterisations calibrated against GCM or process based models tend to underestimate (by a factor of 2-3) the changes when compared to those calibrated against observations.

The SCCM projections of temperature change and sea level rise into the future reflect the underpinning scenario, the basis GCM and the issues noted previously. Table 1 provides a quantitative comparison between the range (due to calibration against a suite of GCMs) from SCCM7 and the *likely*[5] range determined by the IPCC-AR5 (2013) analysis of the GCM simulations for the 4 RCP scenarios. A definitive comparison is not possible as the GCMs, in effect, participating in the comparison need not be the same, nor is the detail of the GCM distribution (from which the IPCC-AR5 quotes) available.

SCCM7 successfully positions the projections for both temperature change and sea level rise for the different RCP scenarios with respect to each other (in order of magnitude and in comparison to the IPCC ranges). The temperature projections from SCCM7 underestimate the upper end of the *likely* range from the IPCC-AR5 (see also Fig. 3 and the accompanying

[5] The term *likely* is used within the IPCC setting to denote a 66-100% probability that the true value lies within the range quoted.

discussion). In contrast, the sea level rise projections from SCCM7 using the parameterisations based on observations ('vermeer' and 'jevrejeva') overestimate both the lower and upper values for the *likely* changes. This is, again, consistent with the difference between observation and model based estimates of sea level rise noted by Grinsted et al. (2010). The possibility of larger values for sea level rise is noted by the IPCC-AR5 (2013) but there is a low confidence and lack of scientific consensus around these higher estimates.

To conclude this section, the temperature calibration technique introduced in Sections 3.1 and 3.2 has been used to quantify the parameters in the temperature response component of SCCM7 against that of 27 GCMs participating in the CMIP5 (Taylor et al. 2012). The calibration illustrates the issues of equifinality in the values of the parameter set obtained (multiple sets of parameter values result in SCCM7 simulations that have similar degrees of an objective measure of success) and the significant correlation of parameter values within the set. SCCM7 is then able to reproduce the main features, magnitudes and approximate uncertainty ranges of the temperature and sea level responses when forced by the four Representative Concentration Pathways in comparison to the IPCC-AR5 analyses. There are systematic differences in the response of SCCM7, in particular an underestimate of the temperature response and an overestimate of sea level rise. These issues can be traced to likely differences in forcing, irreducible uncertainty to the parameter calibration and understood characteristics of the different parameterisation schemes, hence are deemed insufficient to warrant the effort of further investigation at this time.

4 CONCLUSIONS

SCCM is a deterministic model for the globally-averaged carbon cycle and climate system. It comprises representations of the mass balances for the major forcing agents of the Earth's climate together with an energy balance of the Earth system. This report introduces several extensions to SCCM, developing on the previous version described by Harman et al. (2011) and Raupach et al. (2011a). The basis and mathematical formulation for extensions to the carbon cycle representation in SCCM are given alongside those for new components for sea level rise and additional long-lived greenhouse gases. SCCM7 can also be forced by time series of radiative forcing as CO_2-equivalent concentration and run within parameter and uncertainty estimation software PEST.

SCCM – like all (simple) models of the Earth System – requires careful calibration and validation against observations and other, more complex, process-based models. The control experiments from the CMIP5 (Taylor et al. 2012) together with the CO2-eq capability in SCCM7 have been successfully used to provide a) and ensemble of parameter sets for the temperature component of SCCM7 aimed at replicating the CMIP5 GCM suite, b) ensembles of parameter sets for each of these models, recognising that the climate variability simulated by the GCMs will manifest itself as uncertainty in the fitted parameters, and c) ensembles of projections to validate SCCM7 against the CMIP5 models for the 4 RCP scenarios (van Vuuren et al. 2011a). The resulting ensembles of simulations demonstrate i) that multiple combinations

of parameters exist for each GCM (equifinality) and that there is significant correlation between the individual parameters and ii) the simple structure of SCCM does not prevent the generation of a wide range of projections into the future, indeed the range is comparable to that generated by the more complex ESMs and GCMs.

There are several insights which the ensembles of parameter sets and simulations provide – both into the performance of SCCM, the use of simple models and the wider climate system. The issue of equifinality of the calibrated parameter sets is important as it demonstrates the difficulty of separating change and variability within the climate system. The associated significant correlations between parameter values also then illustrates the ease with which incorrect inference can be made if climate variability (and associated statistics) is not accounted for. One particularly important (positive) correlation identified occurs (in SCCM) between the longer time scales in the dataset used to calibrate SCCM and the climate sensitivity. This implies that it is necessary to use long datasets (climate simulations, observations, proxy observations or combinations thereof) to quantify the climate sensitivity (or to calibrate models that use this concept such as SCCM) as the shorter datasets will not adequately resolve the longer time scales and hence underestimate the climate sensitivity.

The performance of the calibrated SCCM7 against the CMIP5 simulations of the RCP scenarios is best described as mixed. SCCM7 is able to correctly position the four scenarios relative to each other. SCCM7 is also able to propagate a reasonable measure of the uncertainty due to the GCM ensemble. There are, however, some systematic biases between the SCCM7 ensemble and the CMIP5 models – with temperature change underestimated and sea level rise overestimated across the four scenarios. The former issue can be explained if we accept that the radiative forcing generated by the CMIP5 differed, e.g. through a different treatment of aerosols, to that used to force SCCM7 in these simulations. The latter issue likely originates from the preeminent use of observations to calibrate the sea-level rise parameterisation scheme and not output process-based models such as those embedded in the CMIP5 models (see Grinsted et al. 2010).

SCCM7 represents a significant advance in capability over SCCM4. On the basis of the results shown, SCCM7 can provide defensible simulations of the global climate across a wide range of scenarios, e.g. for use within Integrated Assessment (Harman et al. 2008; van Vuuren et al. 2011b) or policy analysis. However the issues documented indicate that caution needs to be applied before detailed insights are drawn from SCCM7 parameter values or details of SCCM7 simulations used for the purposes of climate system analysis – at least not without additional effort in the calibration and validation of all components of SCCM. The issues identified also reinforce the need (expectation) for climate change/climate policy analyses to consider, in an adequate and robust manner, the issues of uncertainty, error and variability.

5 REFERENCES

Bi, D., Dix, M., Marsland, S., O'Farrell, S., Rashid, H., Uotila, P., Hirst, A., Kowalczyk, E., Golebiewski, M., Sullivan, A., Yan, H., Hannah, N., Franklin, C., Sun, Z., Vohralik, P., Watterson, I., Zhou, X., Fiedler, R., Collier, M., Ma, Y., Noonan, J., Stevens, L., Uhe, P., Zhu, H., Griffies, S., Hill, R., Harris, C. and Puri, K. (2013) The ACCESS coupled model: description, control climate and evaluation. *Austr. Meteorol. Ocean. J.*, 63(1), 41-64. http://www.bom.gov.au/amm/papers.php?year=2013

Bodman, R.W., Rayner, P.J. and Karoly, D.J. (2013) Uncertainty in temperature projections reduced using carbon cycle and climate observations. *Nature Climate Change*, doi: 10.1038/NCLIMATE1903

Church, J.A., White, N.J., Konikow, L.F., Domingues, C.M., Cogley, J.G., Rignot, E., Gregory, J.M., van den Broeke, M.R., Monaghan, A.J. and Velicogna, I. (2011) Revisiting the Earth's sea level and energy budgets from 1961 to 2008. *Geophys. Res. Let.*, 38, L18601, doi: 10.1029/ 2011GL048794.
http://www.cmar.csiro.au/sealevel/thermal_expansion_ocean_heat_timeseries.html

den Elzen, M.G.J., Schaeffer, M. and Eickhout, B. (2002) Responsibility for past and future global warming: time horizon and non-linearities in the climate system. MNP-report 728001022 (http://www.mnp.nl/en), Netherlands Environmental Assessment Agency (MNP), the Netherlands. http://unfccc.int/methods/other_methodological_issues/items/3546.php

Dix, M., Vohralik, P., Bi, D., Rashid, H., Marsland, M., O'Farrell, S., Uotila, P., Hirst, H., Kowalczyk, K., Sullivan, A., Yan, H., Franklin, C., Sun, Z., Watterson, I., Collier, M., Noonan, J., Rotstayn, L., Stevens, L., Uhe, P. and Puri, K. (2013) The ACCESS coupled model: documentation of core CMIP5 simulations and initial results. *Austr. Meteorol. Ocean. J.*, 63(1), 83–99 http://www.bom.gov.au/amm/papers.php?year=2013

Doherty, J., Muffels, C., Rumbaugh, J. and Tonkin, M. 'PEST: Model-Inpendent Parameter Estimation and Uncertainty Analysis.' www.pesthomepage.org

Enting, I.G. (2007) Laplace transform analysis of the carbon cycle. *Env. Model. Soft.*, 22, 1488-1497 doi: 10.1016/j.envsoft.2006.06.018.

Forster, P., Ramaswamy, V., Artaxo, P., Bernsten, T., Betts, R., Fahey, D.W., Haywood, J., Lean, J., Lowe, D.C., Myrhe, G., Nganga, J., Prinn, R., Raga, G., Schulz, M. and van Dorland, R. (2007) Change in atmospheric constituents and in radiative forcing. In: *Climate Change 2007: The Physical Science Basis. Contribution of Working Group I to the Fourth Assessment Report of the Intergovernmental Panel on Climate Change.* pp.129-234. Cambridge University Press, New York and London.

Gohar, L.K. and Shine, K.P. (2007) Equivalent CO2 and its use in understanding the climate effects of increased greenhouse gas concentrations. *Weather*, 62, 307-311

Good, P., Gregory, J.M. and Lowe, A.J. (2011) A step-response simple climate model to reconstruct and interpret AOGCM projections. *Geophys. Res. Lett.* 38, L01703 doi: 10.1029/2010GL045208, 2011

Good, P., Gregory, J.M., Lowe, J.A. and Andrews, T. (2013) Abrupt CO2 experiments as tools for predicting and understanding CMIP5 representative concentration pathway projections. *Clim. Dyn.*, 40, 1041–1053 doi: 10.1007/s00382-012-1410-4

Gregory, J.M., Ingram, W.J., Palmer, M.A., Jones, G.S., Stott, P.A., Thorpe, R.B., Lowe, J.A., Johns, T.C. and Williams, K.D. (2004) A new method for diagnosing radiative forcing and climate sensitivity. *Geophys. Res. Lett.*, 31, L03205 doi:10.1029/2003GL018747

Grinsted, A., Moore, J.C. and Jevrejeva, S. (2012) Reconstructing sea level from paleo and projected temperatures 200 to 2100 AD, *Clim. Dyn.*, 34, 461-472, doi: 10.1007/s00382-008-0507-2

Gunasekera, D., Ford, M., Heyhoe, E., Gurney, A., Ahammad, H., Phipps, S., Harman, I., Finnigan, J. and Brede, M. (2008) Global Integrated Assessment Model: A new analytical tool for assessing climate change risks and policies. *Australian Commodities*, 15(1), 195-216.

Harman, I.N., Ford, M., Jakeman, G., Phipps, S.J., Brede, M., Finnigan, J.J., Gunasekera, D. and Ahammad, H. (2008) Assessment of future global scenarios for the Garnaut Climate Change Review: An application of the GIAM framework. CSIRO Marine and Atmospheric Research Report. 64pp. http://www.cmar.csiro.au/e-print/open/2008/harmani_a.pdf

Harman, I.N., Trudinger, C.M. and Raupach, M.R. (2011) The Simple Carbon-Climate Model. *Centre for Australian Weather and Climate Research*, Technical Report no 047. http://www.cawcr.gov.au/publications/technicalreports.php 60pp

Haupt, R.L. and Haut, S.E. (2004) *Practical Genetic Algorithms* (2nd Edition). J. Wiley. Hoboken, NJ

IPCC-AR5 (2013) Summary for Policy Makers. In *Climate Change 2013: The physical science basis. Working Group I contribution to the IPCC Fifth Assessment Report*. *36pp.* www.ipcc.ch

Jevrejeva, S., Moore, J.C. and Grinstead, A. (2012) Sea level projections to AD2500 with a new generation of climate change scenarios. *Glob. Planet. Ch.*, 80-81. 14-20. doi: 10.1016/j.gloplacha.2011.09.006

Jones, P.D., Parker, D.E., Osborn, T.J. and Briffa, K.R. (2009) Global and hemispheric temperature anomalies - land and marine instrumental records. *In* Trends: A Compendium of Data on Global Change. Carbon Dioxide Information Analysis Center, Oak Ridge National Laboratory, U.S. Department of Energy, Oak Ridge, Tenn., U.S.A. http://cdiac.esd.ornl.gov/trends/temp/jonescru/data.html
http://www.cru.uea.ac.uk/cru/data/temperature/hadcrut3gl.txt

Joos, F., Bruno, M., Fink, R., Siegenthaler, U., Stocker, T.F., Le Quere, C. and Sarmiento, J.L. (1996) An efficient and accurate representation of complex oceanic and biospheric models of anthropogenic carbon uptake. *Tellus* 48B, 397-417.

Joos, F., Prentice, I.C., Sitch, S., Meyer, R., Hooss, G., Plattner, G-K., Gerbe,r S. and Hasselmann, K. (2001). Global warming feedbacks on terrestrial carbon uptake under the Intergovernmental Panel on Climate Change (IPCC) emission scenarios, *Glob. Biogeochem. Cycles* 15(4), 891-907.

Joos, F., Roth, R., Fuglestvedt, J.S., Peters, G.P., Enting, I.G., von Bloh, W., Brovkin, V., Burke, E.J., Eby, M., Edwards, N.R., Friedrich, T., Frölicher, T.L., Halloran, P.R., Holden, P.B., Jones, C., Kleinen, T., Mackenzie, F.T., Matsumoto, K., Meinshausen, M., Plattner, G-K., Reisinger, A., Segschneider, J., Shaffer, J.G., Steinacher, M., Strassmann, K., Tanaka, K., Timmermann, A. and Weaver, A.J. (2013) Carbon dioxide and climate impulse response functions for the computation of greenhouse gas metrics: a multi-model analysis. *Atmos. Chem. Phys*., 13, 2793–2825 doi: 10.5194/acp-13-2793-2013 www.atmos-chem-phys.net/13/2793/2013/

Joshi, M., Shine, K., Ponater, M., Stuber, N., Sausen, R. and Li, L. (2003) A comparison of climate response to different radiative forcings in three general circulation models: Towards an improved metric of climate change. *Clim. Dyn.*, 20, 843-854 doi:10.1007/s00382-003-0305-9

Knutti, R. and Hegerl, G.C. (2008) The equilibrium sensitivity of the Earth's temperature to radiation changes. *Nature Geoscience.* 1(11), 735-743 doi: 10.1038/ngeo337

Lamarque, J-F., Kyle, G.P., Meinshausen, M., Riahi, K., Smith, S.J., van Vuuren, D.P., Conley, A.J. and Vitt, F. (2013) Global and regional evolution of short-lived radiatively-active gases and aerosols in the Representative Concentration Pathways. *Climatic change*, 109, 191-212 doi: 10.1007/s10584-011-0155-0

L,i S., Jarvis, A.J. and Leedal, D.T. (2009) Are response function representations of the global carbon cycle ever interpretable? *Tellus B*, 61(2), 361-371 doi: 10.1111/j.1600-0889.2008.00401.x

Lindley, D.V. and Scott, W.F. (1996) New Cambridge Statistical Tables, 2nd Edition, Cambridge University Press, UK, 96pp

Meinshausen, M., Raper, S.C.B. and Wigley, T.M.L. (2011a) Emulating atmosphere-ocean and carbon cycle models with a simpler model, MAGICC6 – Part 1: Model description and calibration. *Atmos. Chem. Phys.* 11, 1417-1456, doi: 10.5194/acp-11-1417-2011.

Meinshausen, M., Raper, S.C.B. and Wigley, T.M.L. (2011b) Emulating atmosphere-ocean and carbon cycle models with a simpler model, MAGICC6 – Part 2: Applications. *Atmos. Chem. Phys.* 11, 1457-1471, doi: 10.5194/acp-11-1457-2011

Meinshausen, M., Smith, S.J., Calvin, K., Daniel, J.S., Kainuma, M.L.T, Lamarque, J-F., Matsumoto, K., Montzka, S.A., Raper, S.C.B., Riahi, K., Thomson, A., Velders, G.J.M, and van Vuuren, D.P.P. (2011c) The RCP greenhouse gas concentrations and their extensions from 1765 to 2300. *Climatic Change*, 109(1-2), 213-241 doi**:** 10.1007/s10584-011-0156-z

Raupach, M.R., Canadell, J.G., Ciais, P., Friedlingstein, P., Rayner, P.J. and Trudinger, C.M. (2011a) The relationship between peak warming and cumulative CO_2 emissions, and its use to quantify vulnerabilities in the carbon-climate-human system. *Tellus B*, 63(2), 145-162. doi: 10.1111/j.1600-0889.2010.00521.x

Raupach, M.R., Harman, I.N. and Canadell, J.G. (2011b) Global climate goals for temperature, concentrations, emissions and cumulative emissions. *Centre for Australian Weather and Climate Research*, Technical Report no 042.
http://www.cawcr.gov.au/publications/technicalreports.php 62pp.

Rohling, E.J., Sluijs, A., Dijkstra, H.A., Koehle,r P., van de Wal, R.S.W., von der Heydt, A.S., Beerling, D.J., Berger, A., Bijl, P.K., Crucifix, M., DeConto, R.,[:]Drijfhout, S.S., Fedorov, A., Foster, G.L., Ganopolski, A., Hansen, J., Hoenisch, B., Hooghiemstra, H., Huber, M., Huybers, P., Knutti, R., Lea, D.W., Lourens, L.J., Lunt, D., Masson-Demotte, V., Medina-Elizalde, M., Otto-Bliesner, B., Pagani, M., Paelike, H., Renssen, H., Royer, D.L., Siddall, M., Valdes, P., Zachos, J.C. and Zeebe, R.E. (2012) *Nature*, 491, 683-691 doi: 10.1038/nature11574

Taylor, K.E., Stouffer, R.J. and Meehl, G.A. (2012) An overview of CMIP5 and the experiment design *B. Am. Meteorol. Soc.*, 93(4), 485-498 doi:10.1175/BAMS-D-11-00094.1

Trudinger, C.M., Enting, I.G., Rayner, P.J., Etheridge, D.M., Buizert, C., Rubino, M., Krummel, P.B. and Blunier, T. (2013) How well do different tracers constrain the firn diffusivity profile? *Atmos. Chem. Phys.* 13, 1485-1510, doi: 10.5194/acp-13-1485-2013

Trudinger, C.M., Rayner, P.J., Enting, I.G., Heimann, M. and Scholze, M. (2003) Implications of ice core smoothing for inferring CO2 flux variability, *J. Geophys. Res*. 108(D16), 4492, doi: 10.1029/2003JD003562

Vermeer, M. and Rahmstorf, S. (2009) Global sea level linked to global temperature. *Proc. Natl. Acad. Sci.*, doi:10.1073/pnas.0907765106.

Vermeer, M. and Rahmstorf, S. (2010) Reply to 'Taboada and Anadón: Critique of sea-level rise study invalid'. *Proc. Natl. Acad. Sci*., 107(29), E118. doi:10.1073/pnas.1006678107.

van Vuuren, D.P., Edmonds, J., Kainuma, M., Riahi, K., Thomson, A., Hibbard, K., Hurtt, G.C., Kram, T., Krey, V., Lamarque, J-F., Masui, T., Meinshausen, M., Nakicenovic, N., Smith, S.J. and Rose, S.K. (2011a) The representative concentration pathways: an overview. *Climatic change*, 109, 5-31 doi: 10.1007/s10584-011-0148-z

van Vuuren, D.P., Lowe, J., Stehfest, E., Gohar, L., Hof, A.F., Hope, C., Warren, R., Meinshausen, M. and Plattner, G-P. (2011b) How well do integrated assessment models simulate climate change? *Climatic Change* 104, 255–285 doi: 10.1007/s10584-009-9764-2

Wigley, T.M.L. (1991) A simple inverse carbon cycle model. *Glob. Biogeochem. Cycles*, 5, 373-382.

All CMIP5 GCM data were obtained from the Earth System Grid Federation data portal between the 15-10-2012 and 15-11-2012. http://pcmdi9.llnl.gov/esgf-web-fe/

APPENDIX A: ADDITIONAL VARIABLES AND PARAMETERS IN SCCM7

Table 2 Additional calculated time-varying quantities in SCCM7.

Symbol	Units	Description
C_{TROP}	GtC	CO_2 content in the troposphere
C_{STRAT}	GtC	CO_2 content in the stratosphere
CO2	GtC	(UPDATED) CO_2 content in the atmosphere
X	kt-gas	Perturbation to the content of long-lived gas X in the atmosphere from preindustrial times (nominally CFC11, CFC12, HCFC22, HFC23, HFC134a, SF6, PFC)
SLR	m	globally-averaged sea-level rise
F_{CO2_ST}	GtC y^{-1}	net flux of CO_2 between the troposphere and stratosphere

The first column gives the symbol in the document, the second the units used and the third column gives a description.

Table 3 Additional fixed constants in SCCM7.

Symbol	Value	Units	Description
rM_{HCFC22}	84.468	gHCF22/mol Air	molecular mass of HCFC-22
rMHFC23	70.0138	gHFC23/mol Air	molecular mass of HFC-23
rMHFC134	102.0309	gHFC134a/mol Air	molecular mass of HFC134a
rMPFC14	88.0043	gPFC14/mol Air	molecular mass of PFC-14
rMSF6	146.005	gSF6/mol Air	molecular mass of SF6

The fixed constants are used within SCCM7 to generate the conversion factors between kt of gas and ppb or ppt, in correspondence to the fixed constants $\mathbf{r}_{\mathbf{CFC11\_pptTg}}^{-1}$ in SCCM4. The first column gives the symbol used in this document, the second the fixed value, the third the units used and the fourth column gives a description.

Table 4 New components and changes to existing components in SCCM7.

Comp	Other comps required	State variables
co2	none (uses temp and ch4 if directed to)	co2, ctrop, cstrat, cb1, cb2, cs0, cs1, cs2, cs3, cs4, cs5, cs6, cs7, cs8, cs9
hfc	none	dcfc11, dcfc12, hcfc22, hfc23, hfc134a, pfc14, sf6
temp	none (uses ch4, n2o, cfcs or hfcs if directed to)	temp1, temp2, temp3, slr1, slr2, slr

The first column gives each component name, the second lists other components that must also be chosen and the third column lists the state variables for each component. Note that the SCCM4 module cfcs is duplicated in intent by the new hfc module – consequently only one of these two modules can be run concurrently.

Table 5 Additional SCCM choices.

Comp	Name in code	Defined options
hfc	hfcforchoice	'total' or 'perturbation'
temp	tempmodelchoice	many more options available
temp	slrmodelchoice	'accc','vermeer' or 'jevrejeva'
temp	temphcfc22choice	'modelled' or 'observed'
temp	temphfc23choice	'modelled' or 'observed'
temp	temphfc134choice	'modelled' or 'observed'
temp	temppfc14choice	'modelled' or 'observed'
temp	tempsf6choice	'modelled' or 'observed'
temp	tempdcfc11choice	'modelled' or 'observed'
temp	tempdcfc12choice	'modelled' or 'observed'

The first column gives the relevant component name, the second the choice name in the model code and the third column the options available. See text for further information.

Table 6 Additional SCCM parameters.

Comp	Name in code	Symbol	Typical value	Description
co2	stratfac	f_{STRAT}	0-0.1	fraction of atmospheric CO_2 residing in stratosphere
co2	stratturnover	τ_{STRAT}	4.0	stratospheric turnover time scale (y)
hfc	dcfc11preind	X_{pre}	0	Preindustrial CFC-11 conc. (ppt)
hfc	dcfc12preind	X_{pre}	0	Preindustrial CFC-12 conc. (ppt)
hfc	hcfc22preind	X_{pre}	0	Preindustrial HCFC-22 conc. (ppt)
hfc	hfc23preind	X_{pre}	0	Preindustrial HFC-23 conc. (ppt)
hfc	hfc134preind	X_{pre}	0	Preindustrial HFC-134a conc. (ppt)
hfc	pfc14preind	X_{pre}	0	Preindustrial PFC-14 conc. (ppt)
hfc	sf6preind	X_{pre}	0	Preindustrial SF_6 conc. (ppt)
hfc	dcfc11tauconst	τ_X	45	CFC-11 lifetime (y)
hfc	dcfc12tauconst	τ_X	100	CFC-12 lifetime (y)
hfc	hcfc22tauconst	τ_X	12	HCFC-22 lifetime (y)
hfc	hfc23tauconst	τ_X	270	HFC-23 lifetime (y)
hfc	hfc134tauconst	τ_X	14	HFC-134a lifetime (y)
hfc	pfc14tauconst	τ_X	50000	PFC-14 lifetime (y)
hfc	sf6tauconst	τ_X	3200	SF_6 lifetime (y)
hfc	cfc11radeff	r_{effX}	0.25	radiative efficiency for CFC-11 ($Wm^{-2}ppb^{-1}$)
hfc	cfc12radeff	r_{effX}	0.32	radiative efficiency for CFC-11 ($Wm^{-2}ppb^{-1}$)
hfc	hcfc22radeff	r_{effX}	0.2	radiative efficiency for CFC-11 ($Wm^{-2}ppb^{-1}$)
hfc	hfc23radeff	r_{effX}	0.19	radiative efficiency for CFC-11 ($Wm^{-2}ppb^{-1}$)
hfc	hfc134radeff	r_{effX}	0.16	radiative efficiency for CFC-11 ($Wm^{-2}ppb^{-1}$)
hfc	pfc14radeff	r_{effX}	0.1	radiative efficiency for CFC-11 ($Wm^{-2}ppb^{-1}$)
hfc	sf6radeff	r_{effX}	30.52	radiative efficiency for CFC-11 ($Wm^{-2}ppb^{-1}$)

The first column gives the component name, the second the parameter name in the model code and in this document, the third column gives typical values, the fourth the units used and the fifth column gives a description.

Table 7 Additional SCCM inputs.

Comp	Symbol	Name in code	Description
hfc	F_X	dcfc11emissdata	CFC-11 emissions to be applied in HFC module (kty^{-1})
hfc	F_X	dcfc12emissdata	CFC-12 emissions to be applied in HFC module (kty^{-1})
hfc	F_X	hcfc22emissdata	HCFC-22 emissions (kty^{-1})
hfc	F_X	hfc22emissdata	HFC-23 emissions (kty^{-1})
hfc	F_X	hfc134emissdata	HFC-134a emissions (kty^{-1})
hfc	F_X	pfc14emissdata	PFC-14 emissions (kty^{-1})
hfc	F_X	sf6emissdata	SF_6 emissions (kty^{-1})
temp		tempdcfc11choice	source for dcfc11 time series to be used in the temperature component – 'modelled' or 'observed'
temp		tempdcfc12choice	as above for dcfc12 variable
temp		temphcfc22choice	as above for hcfc22 variable
temp		temphfc23choice	as above for hfc23 variable
temp		temphfc134choice	as above for hfc134 variable
temp		temppfc14choice	as above for pfc14 variable
temp		tempsf6choice	as above for sf6 variable
temp	s_{fhfc}	sfhfc	switch (0 or 1) to apply the radiative forcing from changes in the HFC component gases.

The first column gives the relevant component name and the second the symbol used in the equations. The third column gives the name used in the model code and the fourth column gives a description.

Table 8 Additional SCCM outputs.

Comp	Output	Description
co2	ctrop	CO_2 content of the troposphere (ppm)
co2	cstrat	CO_2 content of the stratosphere (ppm)
co2	co2meth	Carbon flux into the atmosphere due to oxidation of methane (GtC y^{-1})
hfc	dcfc11	CFC-11 concentration from HFC module (ppt)
hfc	dcfc12	CFC-12 concentration from HFC module (ppt)
hfc	hcfc22	HCFC-22 concentration (ppt)
hfc	hfc23	HFC-23 concentration (ppt)
hfc	hfc134	HFC-134a concentration (ppt)
hfc	pfc14	PFC-14 concentration (ppt)
hfc	sf6	SF6 concentration (ppt)
hfc	dcfc11emiss	CFC-11 emissions used in HFC module (kt y^{-1})
hfc	dcfc12emiss	CFC-12 emissions used in HFC module (kt y^{-1})
hfc	hcfc22emiss	HCFC-22 emissions (kt y^{-1})
hfc	hfc23emiss	HFC-23 emissions (kt y^{-1})
hfc	hfc134emiss	HFC-134a emissions (kt y^{-1})
hfc	pfc14emiss	PFC-14 emissions (kt y^{-1})
hfc	sf6emiss	SF6 emissions from (kt y^{-1})
temp	rfhfc	Radiative forcing due to gases in HFC module (Wm^{-2})
temp	co2e	CO2-eq based on all radiative forcing (ppm)
temp	co2er	CO2-eq based on radiative forcing from GHGs only (ppm)
temp	slr	sea-level rise (m)

The first column gives the relevant component name, the second the name of the output quantity in the model code and the third column gives a description.

APPENDIX B: SCCM CALIBRATIONS FOR 27 GCMS

Figure 6 shows the 3-term calibration of SCCM7 against 27 GCMs participating in the CMIP5. These show a wider range of response than the 6 models considered in more detail in Section 3 and the general strength of the calibration technique. There are also weaknesses in some cases. Most examples of weaknesses occur when the calibration systematically underestimates the temperature change one control simulation but overestimates the other control scenario. This general feature cannot be overcome through different choices of parameters and likely originates in nonlinearities or path dependencies in the GCM relationship between radiative forcing and temperature change. Table 9 gives the values for the parameters in the SCCM calibration sets and for the metric *J* for each of the GCMs considered.

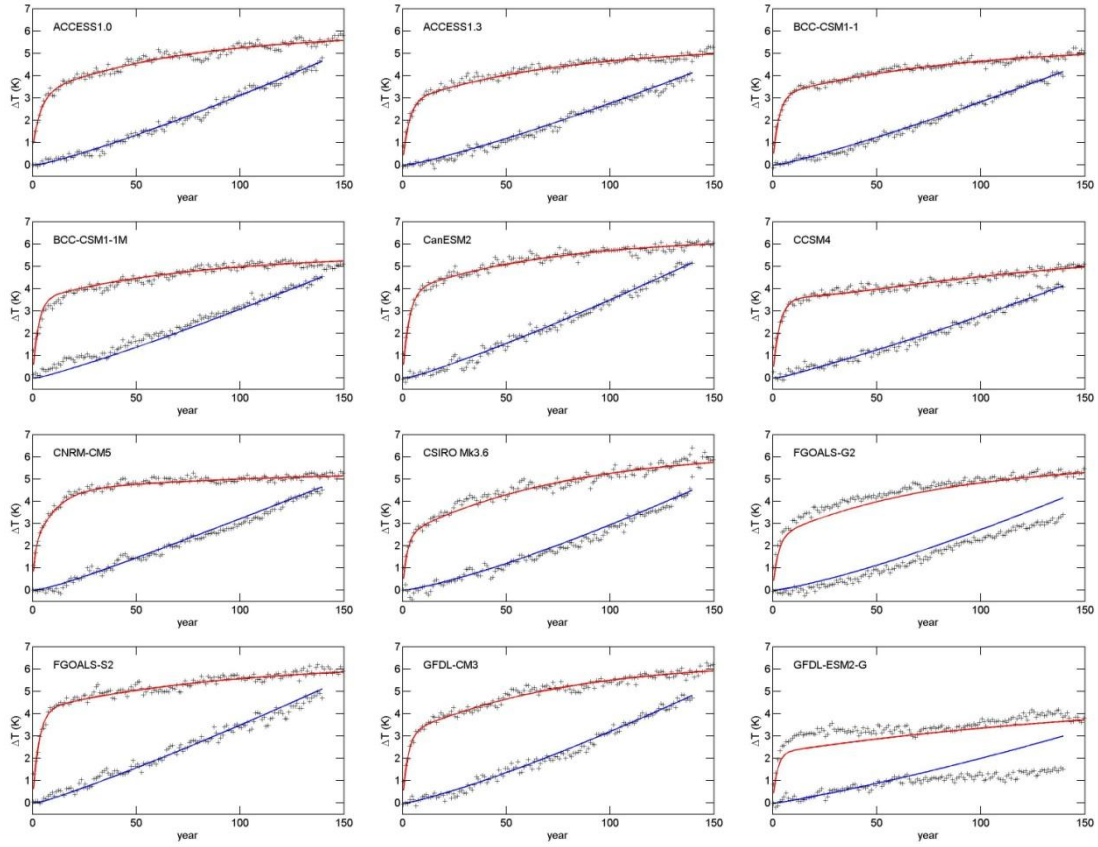

Fig. 6 GCM temperature changes from and fitted response functions to the two control simulations for 27 models from the CMIP5. Crosses show the GCM simulation data and lines show the SCCM7 calibration using all data. Upper lines/crosses refer to the abrupt 4×CO_2 control simulation; lower lines/crosses refer to the 1%-per-year increasing CO_2 simulation. Temperature data from one simulation is used in the calibration process even if the modelling group has undertaken and reported an ensemble of simulations. See Fig. 2 for exemplar cases of the impact of climate variability and the subsequent parameter uncertainty on these calibrations.

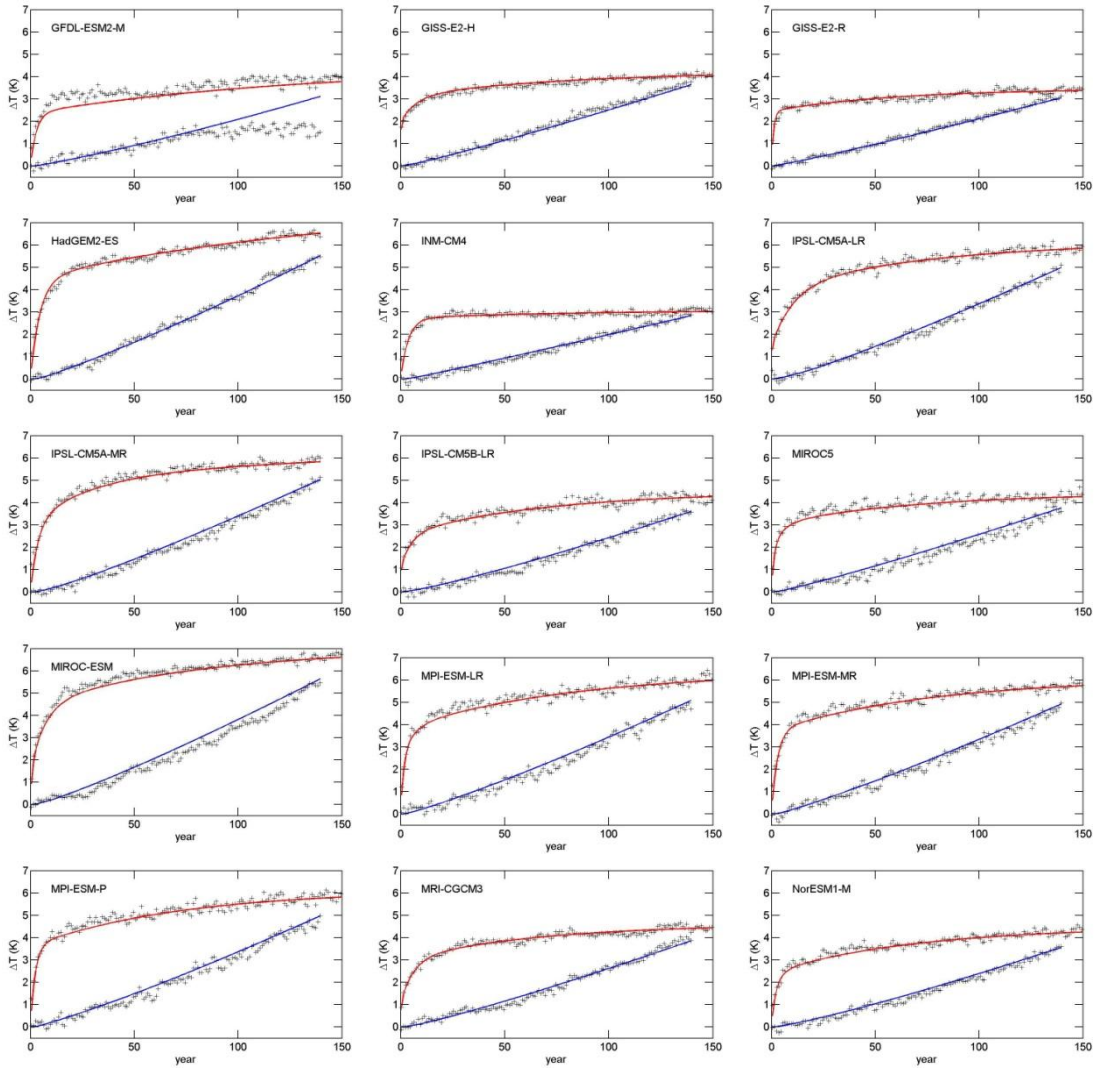

Figure 6 continued. GCM temperature changes from and fitted response functions to the two control simulations for 27 models from the CMIP5.

The calibrations against the GFDL-ESM2-G and GFDL-ESM2-M (and to a lesser extent against the FGOALS-G2) models are particularly poor due to unknown reasons. Figure 7 shows the calibration of SCCM7 when only the data from the abrupt 4×CO_2 control simulation is used. The consequent (significant) mismatch between SCCM7 and the 1%-per-year increasing CO2 control simulation, especially the general character of those data towards the end of the simulation, suggests that the issue originates with the GCM simulations and not with the SCCM calibration.

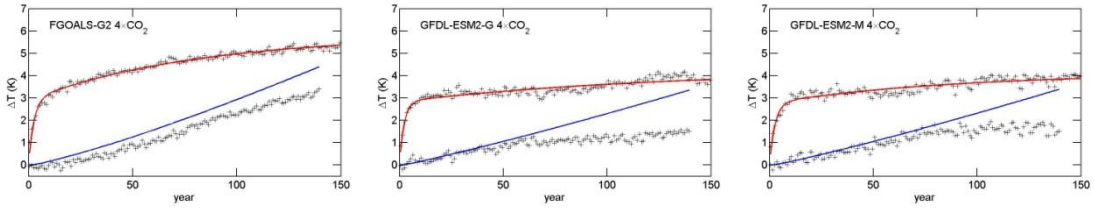

Fig. 7 As Fig. 6 but where only data from the abrupt 4×CO2 control simulation has been used to calibrate the SCCM7 parameters.

Table 9 SCCM7 temperature component parameters for each of the 27 GCMs obtained by calibration against data from both control simulations.

Model	$\Delta T_{2\times}$ (K)	a_1	a_2	a_3	α_1 (y)	α_2 (y)	α_3 (y)	J (K^2)
ACCESS 1.0	2.95	0.13	0.4	0.47	0.2	3.9	29.0	0.024
ACCESS 1.3	2.65	0.53		0.47	3.0		75.0	0.024
BCC-CSM1-1	2.66	0.58		0.42	2.8		84.0	0.015
BCC-CSM1-1M	2.72	0.63		0.37	2.6		69.0	0.043
CanESM2	3.14	0.61		0.39	3.0		69.0	0.026
CCSM4	2.74	0.41	0.22	0.27	1.7	7.1	134.0	0.026
CNRM-CM5	2.71	0.31	0.51	0.18	0.9	9.8	120.0	0.023
CSIRO Mk3.6	3.14	0.39		0.61	2.2		76.0	0.048
FGOALS-G2*	2.83	0.41		0.59	2.4		72.0	0.133
FGOALS-S2	3.13	0.66		0.34	3.0		90.0	0.039
GFDL-CM3	3.22	0.48		0.52	2.6		80.0	0.030
GFDL-ESM2-G*	2.48	0.45		0.55	2.2		190.0	0.325
GFDL-ESM2-M*	2.23	0.53		0.47	2.8		134.0	0.222
GISS-E2-H	2.12	0.47	0.26	0.27	0.3	7.5	80.0	0.014
GISS-E2-R	1.73	0.71		0.29	1.0		61.0	0.011
HadGEM2-ES	3.51	0.60		0.40	4.0		87.0	0.023
INM-CM4	1.54	0.88		0.12	3.6		79.0	0.013
IPSL-CM5A-LR	3.08	0.24	0.41	0.35	0.3	10.1	77.0	0.025
IPSL-CM5A-MR	3.04	0.32	0.35	0.33	1.7	11.8	69.0	0.035
IPSL-CM5B-LR	2.25	0.24	0.33	0.43	0.3	5.0	69.0	0.028
MIROC-ESM	3.51	0.22	0.41	0.37	0.8	6.9	81.0	0.065
MIROC5	2.22	0.43	0.25	0.32	1.2	5.2	70.0	0.050
MPI-ESM-LR	3.20	0.41	0.19	0.40	1.5	6.2	84.0	0.048
MPI-ESM-MR	3.04	0.61		0.39	2.8		76.0	0.036
MPI-ESM-P	3.06	0.59		0.41	2.2		72.0	0.048
MRI-CGCM3	2.31	0.23	0.42	0.35	0.4	6.0	67.0	0.019
NorESM1-M	2.25	0.46	0.09	0.45	2.0	6.4	72.0	0.024

APPENDIX C: ESTIMATION OF RADIATIVE FORCING FROM GCM SIMULATION OUTPUT

Section 3.2 demonstrates the performance of the calibrated SCCM against GCM simulations of the Representative Concentration Pathways scenarios undertaken as part of the CMIP5 (van Vuuren et al. 2011a, Taylor et al. 2012 – see also Fig. 8). The discussion of these results highlighted the possibility that the radiative forcing scenario calculated endogenously by the GCMs may not be the same as that used to drive SCCM in the comparison, given the different treatment of radiative transfer and aerosol forcing between the GCMs and MAGICC. These differences thus represent a hypothesis as to an underlying cause of the dissimilarity in the results shown.

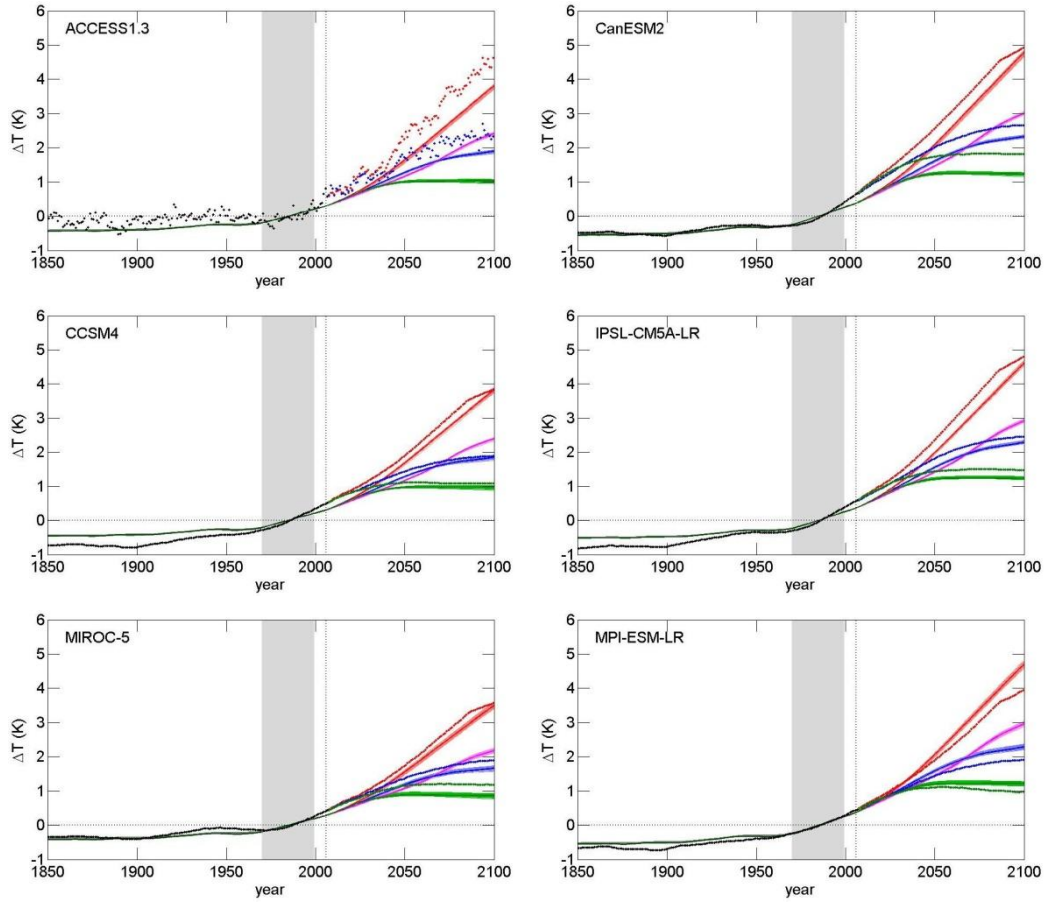

Fig. 8 **(**Fig. 3 repeated) Comparison of SCCM7 projections against full GCM simulations for the available RCP scenarios. Light coloured bands give the range spanned by the SCCM calibration ensemble; darker coloured lines give the projection using the central calibration. Dots give projections from the GCMs themselves - noting that for GCMs other than ACCESS13 the ensemble average of 3-6 simulations is shown (see Section 3.2). Green, blue, magenta and red refer to the RCP3PD, RCP4.5, RCP6 and RCP8.5 scenarios respectively. Black refers to the pre-2006 'historical' scenario which is common to the four RCP scenarios. All simulations are referred to the average over the period 1970-1999 (indicated by the shaded box), hence ΔT in the figures is not that in Eq (C1).

Unfortunately radiative forcing is not readily obtained from GCM output, directly or indirectly, given the multiple timescales acting in the climate system and the difficulty in differentiating between forcing and feedback. Consequently the hypothesis is not easily tested. In this appendix we follow the regression approach of Gregory et al. (2004) to *estimate* radiative forcing from readily available GCM output and compare these estimates with the time series used to force SCCM in the comparison shown in Section 3.2. This forms an independent, but not definitive, method of assessing the hypothesis.

The regression approach uses control scenario GCM simulations to calibrate a linear regression model for the relationship between radiative forcing and temperature change. The regression can then be used to estimate climate system parameters as well as radiative forcing time series for other scenarios (Gregory et al. 2004). The underpinning assumption to the approach is that the change in outgoing radiative flux (across all bands), *H*, is proportional (or close to) the change in globally-averaged near-surface air temperature ΔT from pre-industrial conditions. This assumption has support, being an observed characteristic of many GCMs, however it is highly simplified with known issues (see e.g. Joshi et al. 2003). At global scale and over time scales of years or greater, the net downward heat flux $N=RF-H$, where *RF* is the radiative forcing, is the rate of increase of heat stored in the climate system. We have

$$N(t) = RF(t) - H(t) = RF(t) - \alpha\,\Delta T(t) \qquad \text{(C1)}$$

where α, the climate response parameter with units $Wm^{-2}K^{-1}$, is the proportionality constant. Importantly, for most GCMs, α is found to be roughly independent of both climate state and forcing (Gregory et al. 2004). This implies that α can be estimated from one GCM simulation and then Eq (C1) inverted to estimate *RF* given *N* and ΔT for a different scenario. The abrupt $4\times CO_2$ control scenario is the obvious scenario to base the estimation upon as Eq (C1) is then a linear relationship with two constant parameters and is amenable to simple linear regression.

To implement Eq (C1) in practice both ΔT and *N* are required for the scenarios considered. There is one unanswered question to this point: At what vertical level should *N* be calculated? For full equivalence with the definition of radiative forcing, the appropriate level is at the tropopause[6]. However the tropopause is a continually adjusting boundary making the determination of *N* non-trivial and somewhat arbitrary. Gregory et al. (2004) however also show that the regressed parameters obtained using *N* determined at the top of the atmosphere, N_{TOA}, agree well with those obtained using *N* at the tropopause. As N_{TOA} is routinely reported from GCM simulations this provides a ready method to *estimate* the radiative forcing for arbitrary scenarios without the need for additional simulations.

To illustrate the approach, the left panel of Fig. 9 shows the process of calibrating the regression for the ACCESS 1.3 GCM. Black markers give the data from the first 25 years of the abrupt $4\times CO_2$ control scenario simulation, with the data for the remaining 125 years in blue. The relationship between ΔT and N_{TOA} is approximately linear however there is a statistically significant (and in cases subsequently important) change in slope depending on whether the full data set or only the early period data are used. In principal the earlier parts of the control simulation give the stronger signal for α as the latter parts are impacted by both forcing and feedback (and climate variability provides more relatively more scatter to the data).

[6] as radiative forcing is defined as the 'Change in net downward radiative flux at the tropopause after allowing for stratospheric temperatures to readjust to radiative equilibrium, while holding surface and tropospheric temperatures and state variables fixed at the unperturbed values.' (Forster et al. 2007)

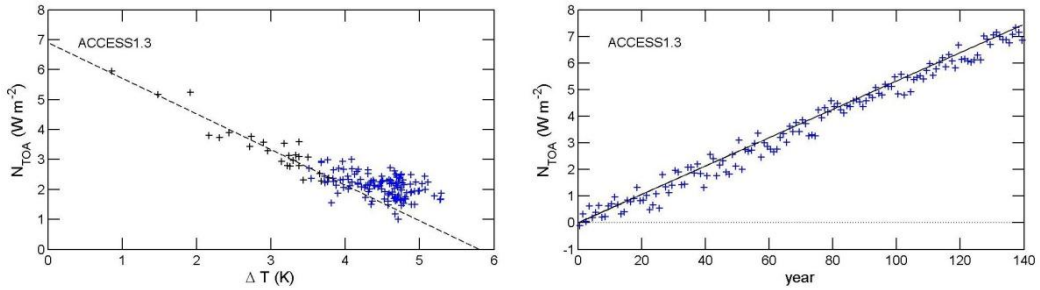

Fig. 9. Left panel: Regression of the annually and globally averaged net radiative flux at the top of the atmosphere against change in near-surface air temperature taken from the ACCESS 1.3 abrupt 4×CO_2 control simulation. Blue markers show data from all years of the simulation, black markers from the first 25 years. Right panel: Time series of the radiative forcing for the 1%-per-year increasing CO2 control simulation. Markers give the radiative forcing obtained from the calibrated Eq (C1), black line gives the analytical solution (Eq 17 with a value of A=5.35 Wm^{-2}).

To test the approach we show the results from calibrated Eq (C1) in inverted form when applied to the 1%-per-year increasing CO_2 control scenario. The right panel of Fig. 9 shows the radiative forcing (markers) as estimated by the regression together with the analytical solution for the radiative forcing for this scenario. The regression method successfully estimates *RF* for this control scenario indicating that, when the radiative forcing is due to CO_2 alone at least, the regression approach can produces plausible estimates for *RF* despite the distinctly different temporal characteristics of the scenarios.

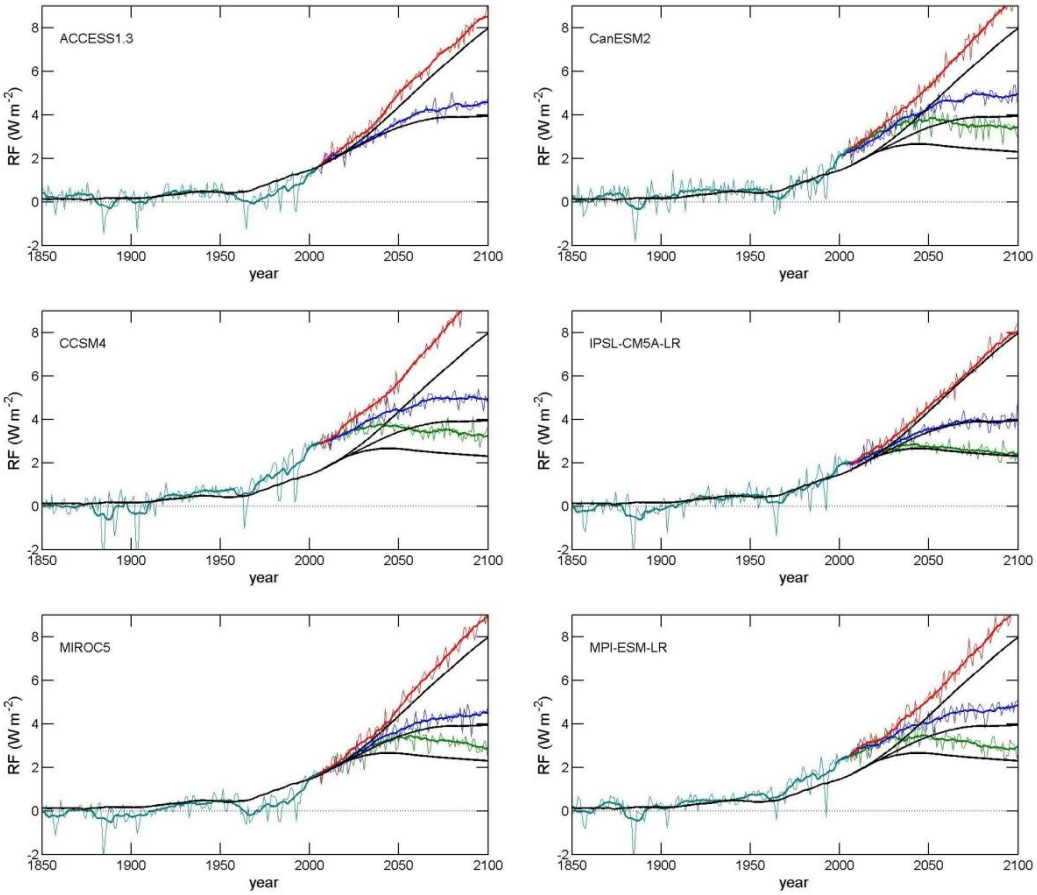

Fig. 10 Comparison between time series of radiative forcing obtained from Eq (C1) and that used to drive SCCM for 6 GCMs and three representative concentration pathway scenarios. Thin coloured lines give the annual time series of the estimated RF for the historical period (cyan), the RCP3PD (green), RCP4.5 (blue) and RCP8.5 (red) RCPs. Thick coloured lines give the 9-year running average of the annual time series. Black lines give the respective RF used to drive SCCM (determined as the RCP CO_2-eq time series with Eq 17 and a value of A=5.35 Wm^{-2}). 25 years of the abrupt 4×CO_2 control simulation were used to calibrate the regression.

Figures 10 & 11 show the resultant comparison between the radiative forcing estimated from the GCM simulations against that used to force SCCM for the 6 GCMs considered in detail in Section 3.2. Figure 10 shows the results when the calibrating regression uses only the first 25 years of the abrupt 4×CO_2 control simulation, whereas Fig. 11 shows the results when all years of the simulation are used. Only one ensemble member is used to generate these estimates (unlike in Fig. 8 where the GCM temperature changes are ensemble averages).

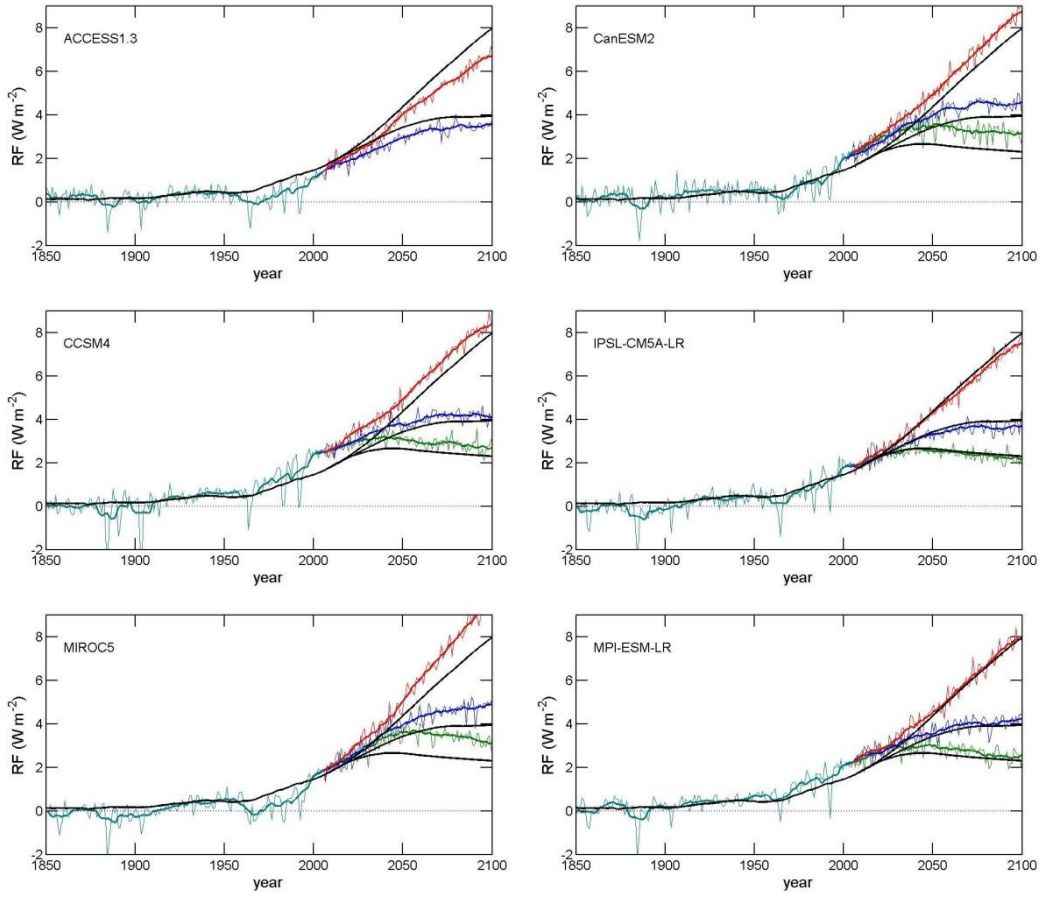

Fig. 11 As Fig. 10 but where all 150 years of data from the abrupt 4×CO_2 control simulation were used to calibrate the regression.

There is qualitative agreement between the estimated radiative forcing and that used to drive SCCM irrespective of the choice of time period upon which to base the regression. The estimates of radiative forcing are in the correct order and in approximately the correct ratios. The quantitative (dis)agreement is similar to that between the SCCM and GCM temperature projections with differences of approximately 0.5-1 Wm^{-2} emerging in most cases around the year 2000. The choice of length of record to calibrate the regression is significant with improved agreement for 3 GCMs but deterioration for 2. These differences can be traced to whether the data from the abrupt 4×CO_2 control scenario are linear (in which case the greater quantity of data assists in accurately quantifying α and hence improvement in performance) or, as in Fig. 9, the later parts of the simulation show a different response (and therefore using the full data set degrades the performance). For the majority of GCM-scenario combinations the differences shown in Figs 10 and 11 are in the correct sense given the temperature projection results in Fig. 8. When SCCM has underestimated the temperature change (compared to the GCM truth) the associated estimate for the radiative forcing from the GCM is greater than used within SCCM (and vice-versa). However this observation does not indicate that it is the radiative forcing that provides the differences between the temperature change projections only that the two results are consistent with each other.

There is particular feature and one general tendency in Figs 10 and 11, however, which do strongly indicate that the radiative transfer components within the GCMs are providing

different values for the radiative forcing than that used in SCCM. During the period 1960-1990 the radiative forcing estimate from the ACCESS 1.3 and MIROC5 models (and to a lesser extent the other models) lies significantly below the SCCM forcing (easiest seen in the 9-year running average). This period is characterised by a series of sharp negative forcing events (likely volcanic eruptions). These events are not included in the RCP forcing time series used to force SCCM. This demonstrates the importance of the aerosol components to the radiative forcing and is particularly important for the (ACCESS1.3) results shown in Fig. 8. The GCM temperature through the reference period does not warm as significantly as SCCM through the period 1960-2000, providing an offset to ΔT and hence impacting the agreement with the SCCM simulations across the full time frame of the scenarios.

The general tendency is that much of the disagreement between in temperature projections and the radiative forcing emerges in the period 2000-2020. This, again, is consistent as the radiative forcing estimates require the use of the temperature change. However during this all of the RCP scenarios undergo a rapid change (reduction) in anthropogenic aerosol loading (van Vuuren et al. 2012). Consequently we would expect differences originating in the radiative transfer components to manifest at this time.

Furthermore there is additional evidence that differences do exist in the radiative transfer components of the GCMs as compared to that of SCCM. The SCCM parameter *A* (Eq 17) can be estimated form the regression as $A = RF_{4\times}/\ln(4)$ where $RF_{4\times}$ is the regressed value of radiative forcing from the abrupt 4×CO_2 control simulation. A default value is *A* = 5.35 $Wm^{-2}K^{-1}$ (e.g. Gohar and Shine 2007). The values obtained through the regressions shown in Figes 10 and 11 range from 4.86 $Wm^{-2}K^{-1}$ (IPSL-CM5A-LR) to 6.27 $Wm^{-2}K^{-1}$ (MIROC5). These estimates are subject to statistical uncertainty[7]; however this large range is indicative of an underlying variation in the effective parameter *A* (or its effective equivalent) between these models[8]. It is important to note that these estimates of *A* are determined from simulations where only the forcing due to CO_2 is included. Extending the suite of gases considered to all those in the RCP scenarios inevitably increases the potential for mismatch between the GCM, MAGICC and SCCM radiative transfer components further.

Together these results indicate two key findings. Firstly, there are subtle, but nevertheless significant differences in the treatment of radiative transfer between the GCMs and that used by MAGICC as used to generate the CO_2-eq time series as used to force SCCM in Section 3.2. The hypothesis therefore has some support but is not proven. Secondly, to accurately reproduce the behaviour of GCMs using SCCM will require substantial effort in tailoring the radiative forcing component of SCCM to each GCM. Given the anticipated usages of SCCM, the inherent variability in climate and variation between GCMs such development is currently not envisaged.

[7] Based on an ensemble of sub-samples of reduced size, the standard deviation of the estimate for *A* is ±0.03 $Wm^{-2}K^{-1}$ for the IPSL-CM5A-LR model and ±0.07 $Wm^{-2}K^{-1}$ for the MIROC5 model.
[8] *A* can be varied in SCCM through the input parameter fco2 (see Table A5 in Harman et al. 2011).

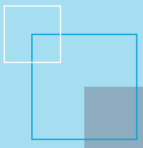

The Centre for Australian Weather and Climate Research is a partnership between CSIRO and the Bureau of Meteorology.